National Defence
Research and Development Branch

Défense nationale
Bureau de recherche et développement

TECHNICAL MEMORANDUM 88/201
January 1988

INFLUENCE OF SPECIMEN SIZE ON FATIGUE CRACK INITIATION OF WELDED HY100 STEEL

Wolfgang Kreuzer

Defence Research Establishment Atlantic

Centre de Recherches pour la Défense Atlantique

Canada

UNLIMITED DISTRIBUTION

National Defence
Research and Development Branch

Défense nationale
Bureau de recherche et développement

INFLUENCE OF SPECIMEN SIZE ON FATIGUE CRACK INITIATION OF WELDED HY100 STEEL

Wolfgang Kreuzer

Wehrwissenschaftliches Institut fur Materialuntersuchungen

January 1988

Approved by L.J.Legget Director/Technology Division

DISTRIBUTION APPROVED BY

D/TD

TECHNICAL MEMORANDUM 88/201

Defence Research Establishment Atlantic

Centre de Recherches pour la Défense Atlantique

Canada

Abstract

The assumption of a statistical distribution of the flaws in a component leads to a prediction of a correlation between crack initiation life and the size of a fatigue loaded part. The influence of the specimen size on the fatigue crack initiation behaviour was analysed for two series of welded HY 100 steel plates of different widths. The weldments were prepared with E12018M2 electrodes.

The applicability of the theory of the statistical size effect was shown in the range of finite endurance. The prediction of the number of cycles to crack initiation and of the allowable stresses for samples of a different size agreed well with the experimental results. (Key words: page 1) →

Résumé

L'hypothèse d'une répartition statistique des fissures dans un élément conduit à l'élaboration d'une corrélation entre la durée d'amorcage d'une fissure et la grandeur d'une pièce soumis à des charges cycliques. L'effet de la grandeur de l'éprouvette sur le comportement de l'amorcage des fissure des fatigue a fait l'objet d'une analyse sur deux séries de tôles d'acier HY100 soudées de différentes largeurs. Les soudures ont été pratiquées a l'aide d'électrodes E12018M2.

L'applicabilité de la théorie de l'effet statistique de grandeur a été démontrée dans la gamme de l'endurance finie. La prédiction touchant le nombre de cycles d'amorcage de fissures et les contraintes admissibles pour des éprouvettes de différentes grandeurs cadre bien avec les résultats expérimentaux.

Acknowledgments

This work was carried out at DREA while the author was on a Defence Research Fellowship offered by the Canadian Departement of National Defence. The author wishes to express his gratitude to Defence Research Establishment Atlantic for supporting this work and acknowledges the good cooperation with Halifax-Dartmouth Industries Limited, who were responsible for the welding procedures.

Table of Contents

List of Symbols

$g(x,y,z)$	function of stress distribution
h, σ_v	constants for distribution of allowable stresses
k	parameter of Wöhler-curve
L/L_o	magnification factor
m, N_v	constants for distribution of the number of cycles to crack initiation
N_i	number of cycles
N_b	predetermined number of cycles
P_{fi}	probability of crack initiation
A/A_o	magnification factor
σ	nominal stress
σ_{max}	maximum stress
σ_{low}	lower stress amplitude
σ_{high}	higher stress amplitude

1. Introduction

Fatigue strength evaluation of welded joints is essential since many fatigue loaded structures are fabricated by welding. The fatigue life of a component is determined by the sum of elapsed cycles required to initiate a fatigue crack and to propagate the crack from a subcritical size to critical dimensions. The behaviour of a cyclically loaded part can be fully understood only when these phases are evaluated individually.

It is well known that surface defects, especially in high strength steels, play an important role in crack initiation under cyclic loading. Since these defects are statistically distributed, fatigue life has a large scatter even if the test conditions are strictly specified. Therefore the crack initiation phase should be analysed from a probabilistic point of view. The statistical theory of the size effect was used successfully in the past to describe the fatigue crack initiation behaviour of homogeneous materials [1,2,3].

The objective of this report is to prove that the same theory is applicable for welded joints. It presents the results of an investigation of the specimen size effect on the fatigue crack initiation behaviour in SMAW weldments of HY 100 plates. The experiments were designed by the boundary technique in the range of finite endurance. Using the theory of the statistical size effect, the scatter of the number of cycles to crack initiation on a certain stress level as well as the allowable stress amplitudes for a given number of cycles could be explained and predicted for plates of different sizes.

2. Theory

2.1. Theory of the Statistical Size Effect

Weibull and others [4,5] developed a model which uses the distribution of defects to describe the scatter of the ultimate strength of brittle materials. Because of the same type of fracture - local crack initiation and fracture without macroscopic plastic deformation - this model was transferred to the fatigue crack initiation behaviour of homogeneous materials [6]. The model assumes that the crack always starts from a surface defect. The crack initiation life of a part is therefore determined by the defect with the lowest resistance against crack initiation (weakest-link-concept). Considering the statistical distribution of the defects in a material, the scatter of the number of cycles N_i to generate a crack of a threshold size can be described by the Weibull-formula

$$P_{fi} = 1-\exp\left[-(N_i/N_v)^m\right] \qquad (1)$$

where P_{fi} is the probability of crack initiation and N_v and m are constants.

Since the probability to find a large defect is higher in a large surface than in a small one, the average crack initiation life of a series of large samples should be shorter than that of smaller ones tested under the same conditions [7]. To compare geometrically similar parts equation 1 has to be extended with the magnification factor A/A_o.

$$P_{fi} = 1-\exp\left[- A/A_o(N_i/N_v)^m\right] \qquad (2)$$

A and A_o are the loaded surface areas of the different parts.

The size of the highly loaded area in a fatiguing part depends also on the stress distribution and concentration around notches. The highly loaded area in a sample with a sharp notch will certainly be smaller than in an unnotched or only slightly notched specimen. Therefore, if one applies the same maximum stress, the average crack initiation life of notched specimens should be longer than that of unnotched ones. To account for the non-uniform stress distribution

$$\sigma = \sigma_{max}\, g(x,y,z) \qquad (3)$$

the probability of failure must be stress weighted.

$$P_{fi} = 1-\exp\left\{-1/A_o(N_i/N_v)^m \int \left[g(x,y,z)\right]^h dA\right\} \qquad (4)$$

Using these formulas, it is possible to predict the fatigue initiation life of parts of different size and shape for a given stress from the test results of only one type of sample. As a corollary it is possible using equations (5), (6) and (7) to predict the allowable stress levels for specimens with different sizes and shapes with predetermined fatigue lives.

$$P_{fi} = 1-\exp\left[-(\sigma/\sigma_v)^h\right] \qquad (5)$$

$$P_{fi} = 1-\exp\left[-A/A_o(\sigma/\sigma_v)^h\right] \quad (6)$$

and

$$P_{fi} = 1-\exp\left\{-1/A_o(\sigma_{max}/\sigma_v)^h\int\left[g(x,y,z)\right]^h dA\right\} \quad (7)$$

where σ is the nominal stress, σ_{max} is the maximum stress in the notch tip and σ_v and h are parameters.

A detailed deriviation of these formulas can be found in [1] and [8].

2.2. The Boundary Technique in the Range of Finite Endurance

In order to prove the applicability of the theory for welded joints an experimental method which gave statistically reliable results had to be used. The tests were therefore designed by the boundary technique in the range of finite endurance, which is a specimen-saving method for the evaluation of specific values in this range [9]. It enables one to evaluate the allowable stress of defined probability of failure at a predetermined number of cycles N_b as well as the distribution of the number of cycles to crack initiation at two given stress levels.

This technique starts with a test at a stress level that is expected to lead to crack initiation at N_b cycles (Figure 1). This test can have only two results: failure or no failure before N_b cycles. The next samples are, depending on

the result, tested at gradually higher or lower stress levels until the opposite result of the first test occurs. Half of the samples are tested at this first stress level. The probability of failure at this level and the slope of the Wöhler-curve determine the distance to the second stress level. The information about the slope of the Wöhler-curve can come either from former tests or the literature. For a good statistical analysis of the data both stress levels should lie as far apart as possible in a given scatter band (e.g. 10%-90% probability of failure). Depending on the stress level which was found first, one of these two formulas is used to find the second stress level:

$$\log\varnothing_{low} = (\log N_{xhigh} - \log N_b)/k + \log\varnothing_{high} \qquad (8)$$

$$\log\varnothing_{high} = (\log N_{xlow} - \log N_b)/k + \log\varnothing_{low} \qquad (9)$$

$\varnothing_{high,low}$ are the stress levels, $N_{xhigh,low}$ are the number of cycles for a defined probability of failure x, and 1/k is the slope of the Wöhler-curve.

After finishing the tests with the rest of the samples at the second stress level, the distribution of the number of cycles to crack initiation at both stress levels (horizontal analysis) as well as the allowable stress of any probability of failure at N_b cycles (vertical analysis) can be determined. In this study the 2-parameter Weibull-formula was used in both cases. The parameters N_v and m for the distribution of the crack initiation lives were determined with a computer program using the Likelihood-method.

From this analysis one gets two couples of values,

(P_{f1}, σ_1) and (P_{f2}, σ_2), which mark the probability of failure for N_b cycles (P_{fi}) on each stress level (σ_i). Using equation 5 the two parameters σ_v and h of the distribution function for the fatigue strength at N_b cycles can be determined with

$$k = \frac{\ln(-\ln(1-Pf2)) - \ln(-\ln(1-Pf1))}{\ln\sigma_2 - \ln\sigma_1} \qquad (10)$$

$$\sigma_v = \exp\{\ln\sigma_1 - [\ln(-\ln(1-P_{f1}))]/h\} \qquad (11)$$

With these formulas the distribution function is known and the allowable stress $\sigma(P_{fi})$ of any probability of failure for N_b cycles can be calculated with

$$\sigma(P_{fi}) = \exp\{\ln\sigma_v + [\ln(-\ln(1-P_{fi}))]/h\} . \qquad (12)$$

This additional vertical analysis of the data in the range of finite endurance gives more information than the simple horizontal analysis of the two stress levels and very often allows a certain correction of the Wöhler-curve in this range.

3. Material and Experimental Work

3.1. Material

The tests were performed with 25 mm thick plates of HY 100. The steel was certified to meet the requirements of MIL-S-16216J(SH) for grade HY 100 steel. The chemical composition and mechanical properties are shown in Tables I and II. The electrodes used in this project originated from Alloy Rods and were certified to meet the requirements of MIL-E-0022200/10A(SH) for MIL-12018-M2 Class 1 electrodes. Two sizes were used and the chemistry and mechanical properties can be found in Tables III and IV.

3.1.1. Welding Procedure

Six plates, 1500 mm x 300 mm, were welded in the flat position to give three complete weldments [10]. The plates were cut out by oxy-acetylene flame cutting and squared by machining approximately 2 mm from the burned surface to remove any heat affected zone. The test bevels were prepared with a double Vee groove (60°) with a 1/3 - 2/3 offset.

The plates were slowly brought up to the minimum preheat temperature of 100°C. The electrodes were baked at 400°C - 475°C for three hours prior to being used. The pass sequence used is shown in Figure 2. The first three passes on each side were deposited with a 3.2 mm diameter electrode with a heat input of 1.77 kJ/mm. All subsequent passes were deposited with a 4 mm diameter electrode also with a heat input of 1.77 kJ/mm. Side two of the welded test plates was backgouged by grinding to sound metal, and magnetic particle inspection was used to ensure that the gouged groove was crack

free.

After welding, the minimum preheat temperature was maintained for at least four hours. After the plates had cooled to room temperature, they were left for a minimum of 72 hours before being radiographed for compliance with the ASME Boiler and Pressure Vessel Code Section VIII. The plates were also ultrasonically tested for compliance with D.G. Ships/PS/9022-C and D.G. Ships/G/10000 B. All plates were found to be free of unacceptable defects. All welds were also of acceptable quality. Examples of all three weldments are shown in Figures 3 to 5.

3.1.2. Metallography

Samples, transverse to the welding direction, were cut from approximately the center of each plate for metallographic examination. The macrographs of three plates are shown in Figures 6 to 8. The welds were symmetrical with a narrow heat affected zone (HAZ) of about 3mm. The weldment in plate 3 showed a misalignment of 1.2 mm. A little undercut (0.3 mm) was found in several locations. The macrographs did not reveal the presence of any cracks, confirming the results from NDT. In plate 1 a little pore which is not relevant to the fatigue crack initiation was found in the weld metal. In the macrographs of plates 1 and 3, which were made after the test, three fatigue cracks can be seen. All three weldments had the same microstructure (Figure 9): 90% of the microstructure in the weld metal was fine, acicular ferrite with a minimum of coarse polygonal or proeutectoid ferrite. The HAZ showed a mainly bainitic-martensitic structure.

Knoop microhardness (500 g) traverses were made across

the weld zone. The diagrams (Figures 10 - 12) show little difference between the three weldments. The base metal hardness was found to be 250 KN_{500}. The maximum hardness occurring in the HAZ was between 350 KN_{500} and 380 KN_{500} for all plates. The hardness in the weld metal varied from 200 KN_{500} to 330 KN_{500} with the highest values near the fusion line.

3.1.3. Preparation of the Samples

The samples of two different widths (75 mm and 150 mm) were saw cut according to Figure 13. To avoid any influence of inhomogeneties in the parent material, the wide and narrow samples were cut out of the plates in random sequence. After cutting, the edges were rounded with a radius of 12 mm by machine grinding. The final grinding, especially around the weldments, was done by hand with 400 grit sandpaper.

3.2. Experimental Procedure

The test device needed for this study had to be capable of performing fatigue tests on heavy plates of different sizes up to high loads. Considering the equipment available at DREA, a 4-point-bending test was determined to be most suitable. For the tests a servohydraulic testing machine (Instron 1335, 1000 kN) was used. The general set-up for the test is shown in Figure 14.

The tests were performed under load control with a frequency of 2 Hertz. For static strain measurements on the surface of the samples, the load, stroke and strain signals could be displayed on the readout module and recorded with an x-y recorder. To make sure that each sample was loaded with the same stress, strain measurements were made with strain gauges or an extensometer on each sample. During the dynamic test, the stroke and load signals were monitored with a Tektronix 4052.

To determine the point of crack initiaton, the expected number of cycles for the test was divided into 1000 steps. At the end of every step the computer determined the maximum and the minimum values for the load and stroke signals and displayed them as a function of the number of elapsed cycles on the screen. The data were stored on a magnetic tape for further analysis. Changes in the stroke signal, which was nearly identical with the deflection of the sample under the two inner rollers, reflected variations in the resistance of the sample against bending. This change meant, if all other test conditions were constant, a decrease of the cross section caused by a crack, and could be used for the determination of crack initiation. To obtain good results with this technique it was very important that the applied load be constant and that the sample be held motionless on the bending jig during the test. Recordings of the test results are shown in the Appendix.

4. Results

4.1. Unwelded Plates

To check the suitability of the experimental procedure some tests were first conducted on unwelded plates. The applied stress of 900 MPa was chosen to obtain crack initiation at around 90000 cycles. It was possible to determine small changes of the deflection (<0.05 mm) reliably. That meant that the cracks could be detected in an early stage of crack growth. The results are shown in Table V. The tests were continued until the change of the deflection reached 2 mm. At this stage all plates showed more than one crack.

Since in a 4-point-bending test the stress between the two inner rollers is theoretically constant, the distribution of the crack initiation points on the plate verified the quality of the test device. The cracks should be randomly distributed over the whole surface between the two inner rollers.

The cracks were concentrated under the two rollers in all samples along their longitudinal axes. This agreed with the measurements of the strain distribution on the surface of the samples. The stress was not equal between the two inner rollers, as theoretically expected for the 4-point-bending test, because of the warping of the samples; the stress maximum was always found under one of the two rollers. The maximum difference in the stress was 10%. However, because the weld was in the middle of the two rollers and could be loaded in each test in the same way, the difference in the stress under the rollers did not affect the test results.

More important was the distribution of the crack

initiation points over the width of the samples. The cracks were nearly equally distributed in this direction, as Figure 15 shows. This proved that the test device applied the load equally and that the preparation of the samples avoided any edge effect on the results.

4.2. Welded Plates

In the welded plates all cracks started at the weld toe. Most of the cracks were found in the heat affected zone close to the fusion line (Figure 7). In some samples the cracks originated in the weld metal. In these samples the transition between the base metal and the weld metal was very flat. The location with the highest stress concentration was shifted into the weld metal (Figure 6). The cracks started randomly either on the left or right side of the weld metal and were statistically distributed over the width of the plates (Figure 16, 17). Some plates had cracks on both sides of the weld (Figure 18).

4.2.1. 75 mm Wide Plates

The tests were made using the boundary technique in the range of finite endurance according to section 2.2 with N_b = 90000 cycles. The stress ratio was $\sigma_{low}/\sigma_{high}$ = 0.28. The first sample was tested with a stress amplitude of 475 MPa and showed a crack after 22900 cycles. Decreasing the stress amplitude stepwise by 25 MPa, the third sample failed after 122400 cycles. The first stress level was set to 425 MPa. To find the second stress level the standardized Wöhler-curve for weldments of mild steels [11] was used. This was considered

reasonable because according to results found in the literature [12] for HY 80 this Wöhler-curve seemed to fit the HY steels. Using equation 8 with x = 30% and k = 3.5 the second stress level was determined to be 375 MPa. The results of the individual tests are shown in Table VI.

The horizontal analysis according to section 2.2 gave the following results:

$$425 \text{ MPa: } P_{fi} = 1-\exp[-(N_i/78868)^{3.23}] \qquad (13)$$

$$375 \text{ MPa: } P_{fi} = 1-\exp[-(N_i/167455)^{2.38}] \qquad (14)$$

The parameters h and σ_v were determined using equations 10 and 11 for the vertical analysis.

$$P_{fi} = 1-\exp[-(\sigma_i/413)^{15.22}] \qquad (15)$$

If one assumed that the horizontal analysis as well as the vertical analysis had the same importance, the Wöhler-curve shown in Figure 19 could be drawn with the corrected parameters k and $\sigma_{x\%}$ from Table VIII.

4.2.2. 150 mm Wide Plates

To obtain comparable results the 150 mm wide samples were tested at the same stress levels as the narrow ones. The results are shown in Table VII. Using the same procedure as in

4.2.1 the final results were the following:

horizontal analysis

425 MPa: $P_{fi} = 1-\exp[-(N_i/64666)^{4.15}]$ (16)

375 MPa: $P_{fi} = 1-\exp[-(N_i/111510)^{2.91}]$ (17)

vertical analysis

$P_{fi} = 1-\exp[-(\sigma_i/390)^{16}]$ (18)

The Wöhler-curve is shown in Figure 20.

A complete summary of all important results of the statistical analysis can be found in Table VIII. At the 425 MPa-stress level the mean crack initiation life $N_{50\%}$ of the 75 mm wide samples was 19% higher than of the 150 mm wide samples. For the samples tested at the 375 MPa stress level the difference of $N_{50\%}$ was 46%. The allowable stress amplitude $\sigma_{50\%}$ increases 6% for the narrow samples. A comparison of the two Wöhler-curves is shown in Figure 21. It can be seen that the size effect was bigger than the 10% - 90% scatter band.

5. Discussion

5.1. Prediction of the Number of Cycles to Crack Initiation

Since in this study the weldments of all plates had the same shape, the lengths L and L_o of the weldments were the only parameters which described the difference between wide and narrow plates. Therefore the equations 2 and 6 could be used to describe a possible size effect. They were simplified to

$$P_{fi} = 1-\exp[-L/L_o(N_i/N_v)^m] \qquad (2a)$$

$$P_{fi} = 1-\exp[-L/L_o(\sigma_i/\sigma_v)^h] \qquad (6a)$$

Using equation 2a, 13, 14 and the magnification factor $L/L_o = 150/75$ the two formulas for the prediction are:

$$425 \text{ MPa: } P_{fi} = 1-\exp[-150/75(N_i/78868)^{3.23}] \qquad (19)$$

$$375 \text{ MPa: } P_{fi} = 1-\exp[-150/75(N_i/167455)^{2.38}] \qquad (20)$$

The Figures 22 and 23 show the frequency distribution of the test results with the fitted distribution functions, equations (13) and (14) for the narrow samples and the predicted distribution functions, equations (19) and (20) for the wide samples.

In spite of the relatively small number of samples for statistical analysis, the prediction for the lower stress level (375 MPa) agrees well with the test results. The size effect (46%) can be clearly seen. The predicted mean value $N_{50\%}$ = 107300 was only 9% higher than the test result.

The size effect in the higher stress level (425 MPa) was smaller (19%). The predicted mean value $N_{50\%}$ = 56800 was 4% lower than the test result. The prediction describes the test results very well, especially if one considers that only six 150 mm wide samples were tested. However, because the size effect was smaller and the deviation of the test results from the theoretical Weibull-Distribution therefore more striking, the difference cannot be seen as clearly as in the lower stress level. A comparison of the predicted Wöhler-curve with the test result is shown in Figure 24.

5.2. Prediction of the Allowable Stress Amplitude

For the prediction of the allowable stress amplitude at 90000 cycles the results of the tests at both stress levels were used. Therefore the calculation should be more reliable and accurate than the prediction of the number of cycles to crack initiation at the individual stress levels. With equation 6a, 15 and the magnification factor L/L_o = 150/75 the behaviour of the wide samples can be predicted with

$$P_{fi} = 1-\exp[-150/75(\sigma_i/413)^{15.22}]. \qquad (21)$$

The individual values with a probability of failure of 10%, 50% and 90% are shown in Table IX.

The very good agreement between prediction and test results (difference of the median values <1%) is also demonstrated in Figure 25, which shows the distribution of the allowable stresses for the 75 mm and 150 mm wide plates together with the distribution predicted by equation 21 for the 150 mm sample.

5.3. Examination of the Fracture Surfaces

From the examination of the fracture surfaces it was found that there were a number of randomly distributed initial cracks along the weld toe. The small cracks, as they grew deeper, joined into a single almost straight fronted crack. The number and location of these cracks depended on the applied stress (Figure 26, 27).

The density of the initial cracks was lower in the samples which were tested at the 375 MPa-stress level. This was reasonable because only the more severe defects caused crack initiation at the lower stress level. The 150 mm wide samples had an average of 9.6 initial cracks compared with 6.9 initial cracks in the samples tested at the 375 MPa-stress level. The same behaviour was found for the narrow samples. There the ratio between the initial cracks was 5.7 : 3.5. The samples which were tested at the 425 MPa-stress level also showed more initial cracks on both sides of the weld metal (5 : 2).

The importance of the size effect depends on the density of defects in the material. The size effect will be strong when the density of defects is low. Then the

probability of finding a defect severe enough to create a crack depends more on the size of the part. On the other hand, if theoretically the density of the defects is high enough that a severe defect can be found in any small and large part with a probability of 100%, no size effect should be seen.

The test results of this study agree with this consideration. At the 425 MPa-stress level the density of initial cracks was 40% higher than at the 375 MPa-stress level. The effect of specimen size on the mean value of the fatigue life at the 375 MPa-stress level was twice as strong as at the 425 MPa-stress level.

6. Conclusions

Four point bending tests were conducted to investigate the fatigue crack initiation behaviour of welded HY 100 steel plates of two different sizes in the range of finite endurance. The applicability of the statistical theory of the size effect was shown. Overall, the predicted results agreed well with the experimental data: the effect of specimen size on fatigue life was estimated correctly and the examination of the fracture surfaces confirmed the theoretical assumptions of a statistical variation in the severity of potential fatigue initiation sites.

7. References

[1] Böhm,J. "Zur Vorhersage der Dauerschwingfestigkeiten ungekerbter und gekerbter Bauteile unter Berücksichtigung des statistischen Grösseneinflusses", Diss. TU München (1980)

[2] Heckel,K. "Experimentelle Untersuchung des statistischen Grösseneinflusses im Dauerschwingversuch an ungekerbten Stahlproben", Z.f.Werkstofftechnik 6 (1975), 52-54

[3] Ziebart,W. "Ein Verfahren zur Berechnung des Kerb- und Grösseneinflusses bei Schwingbeanspruchung", Diss. TU München (1980)

[4] Weibull,W. "A Statistical Theory of the Strength of Material", IVA Stockholm, Handlingar 151 (1939)

[5] Freudenthal,A. "Statistical Approach to Brittle Fracture", Vol.II, 591-619, Acad. Press New York (1968)

[6] Freudenthal,A. Gumbel,E.J. "On the Statistical Interpretation of Fatigue Tests", Proc. of the Royal Soc. 216 (1953), 309-332

[7] Köhler,J. Heckel,K. "Scatter and Statistical Size Effect at the Fatigue Behaviour of Metallic Specimens", Proc. 2nd Int. Conf. on Mech. Beh. of Mat. 1976, Boston, Spec.Vol. 193-211

[8] Schweiger,G. "Statistischer Grösseneinfluss bei unregelmässiger Schwingbeanspruchung", Diss. HSBW München 1983

[9] Maennig,W.W. "The Boundary Technique in the Range of Finite Endurance", Z.Materialprüfung 27 (1985), 216-222

[10] R.Robichaud Campbell,I. Kreuzer,W. "Shielded Metal Arc Welding of HY 100 Steel Plate with E12018M2 Electrodes", DREA TC/87/310, May 1987

[11] Haibach,E. "Schwingfestigkeitsverhalten von Schweissverbindungen", VDI-Berichte Nr.268 (1976), 179-192

[12] Kazi,H.A. "Effect of Weld Stress on the Fatigue Life of HY 80 Plate", DREA Contract Report CR 87/417 Apr. 1987, unpublished manuscript

8. Tables

Table I

Chemical analysis of HY 100 steel plate

Material or Specification	Elements in % by weight										
	C	Mg	P	S	Si	Ni	Cr	Mo	Va	Ti	Cu
HY 100 [1]	0.14	0.27	0.005	0.007	0.28	2.55	1.40	0.36	0.001	0.001	0.16
MIL-Spec.	0.10-0.22	0.10-0.45	< 0.02	< 0.02	0.12-0.38	2.18-3.37	0.94-1.86	0.17-0.63	< 0.03	< 0.02	< 0.25

1)

from Certification Phoenix Steel Corporation, 16.August 1982 TY II, HY-100

Table II

Mechanical Properties of HY 100 steel plate

Material or Specification	Tensile Strength in Mpa	Yield Strength in Mpa	Elongation in %	Reduction of Area in %
HY 100 [1]	778	694	45	65
MIL-S-16216J(SH)	2)	690-790	> 18	> 45

1) from Certification Phoenix Steel Corporation, 16.August 1982 TYII, HY-100

2) to be recorded for information only

Table III

Chemical analysis of electrodes E12018M2

Electrodes or Specification	Elements in % by weight								
	C	Mg	Si	P	S	Cr	Ni	Mo	Va
E12018M2 3.2 mm [1]	0.03	1.43	0.19	0.017	0.007	0.06	3.58	0.27	0.01
E12018M2 4 mm [1]	0.03	1.19	0.24	0.014	0.011	0.03	3.51	0.57	0.0
MIL-E-0022200/10A(SH)	< 0.10	0.80-1.85	< 0.65	< 0.03	< 0.012	< 0.65	1.50-4.00	< 0.90	< 0.05

1) from Alloy Rods Corporation Certification of Quality Conformance Test No. 2-7430-02 and 2-7431-01

Table IV

Mechanical properties of electrodes E12018M2

Electrodes or Specificatin	Tensile Strength in MPa	Yield Strength in MPa	Elongation in %	Reduction of Area in %
E12018M2 1/8" [1]	845	748	18	63
E12018M2 5/32" [1]	793	714	19	58
MIL-E-0022200/10A(SH)	-	700-785	> 18	-

1) from Alloy Rods Corporation Certification of Quality Conformance Test No. 2-7430-02 and 2-7431-01

Table V

Test results of unwelded plates

stress amplitude = 900 MPa, stress ratio = 0.28

Sample No.	Number of cycles to crack initiation	Number of initial cracks
1	108000	2
2	127000	7
3	77500	3
4	66600	3
5	77000	2
6	90500	4

Table VI

Test results of 75 mm wide welded plates

Sample No	Stress Amplitude in MPa	Number of cycles to crack initiation	Number of initial cracks
1.3	375	162000	4r
1.8	375	124300	3r
3.1	375	67600	3l
3.7	375	81000	4r
3.11	375	122100	5r
3.13	375	106500	5l
5.1	375	198700	3l
5.2	375	171700	3r
5.8	375	297000	1r
1.4	425	122400	4r
1.7	425	72100	9r
3.4	425	58500	4r,5l
3.5	425	82300	4l
3.8	425	67100	5r
5.10	425	53000	5l
5.11	425	46400	4l
5.14	425	64900	5r
5.12	450	58500	4r
3.3	475	22900	5l

r: crack initiation on the right side of the welding seam

l: crack initiation on the left side of the welding seam

Table VII

Test results of 150 mm wide welded plates

Sample No.	Stress Amplitude in MPa	Number of cycles to crack initiation	Number of initial cracks
1.1	375	168500	3l
1.5	375	123500	1l,2r
3.2	375	61300	10l
3.9	375	68000	6r
3.12	375	63000	9l
3.14	375	79300	4l,2r
5.3	375	134200	11l
5.13	375	95200	7l
1.6	425	57300	10r,2l
3.6	425	46700	11r
3.10	425	45100	9l,4r
5.4	425	79300	5r
5.5	425	79700	9r
5.9	425	43700	7r,5l

r: crack initiation on the right side of the welding seam

l: crack initiation on the left side of the welding seam

Table VIII

Statistical analysis of the test results

		75 mm wide samples		150 mm wide samples	
		375 MPa	425 MPa	375 MPa	425 MPa
	$N_{10\%}$	64711 cycles	39300 cycles	55000 cycles	37600 cycles
	$N_{50\%}$	143600 cycles	70400 cycles	98400 cycles	59200 cycles
Horizontal	$N_{90\%}$	237600 cycles	104800 cycles	148400 cycles	77597 cycles
Analysis	$\sigma_{10\%}$	346 MPa		299 MPa	
	$\sigma_{50\%}$	407 MPa		383 MPa	
	$\sigma_{90\%}$	433 MPa		414 MPa	
Vertical	$\sigma_{10\%}$	357 MPa		339 MPa	
	$\sigma_{50\%}$	403 MPa		381 MPa	
Analysis	$\sigma_{90\%}$	437 MPa		411 MPa	
$\sigma_{10\%}$		351 MPa		319 MPa	
	$\sigma_{50\%}$	405 MPa		382 MPa	
Corrected	$\sigma_{90\%}$	435 MPa		413 MPa	
Values	$k_{10\%}$	3.9		3.0	
	$k_{50\%}$	5.6		4.0	
	$k_{90\%}$	6.5		5.2	

Table IX

Prediction of the number of cycles to crack initiation and allowable stress amplitudes

		Predicted Values	Deviation from Test Result
425 MPa	$N_{10\%}$	31700 cycles	-16 %
	$N_{50\%}$	56800 cycles	-4 %
	$N_{90\%}$	84600 cycles	+9 %
375 MPa	$N_{10\%}$	48400 cycles	-12 %
	$N_{50\%}$	107300 cycles	+9 %
	$N_{90\%}$	177600 cycles	+19 %
	$\sigma_{10\%}$	335 MPa	+5 %
	$\sigma_{50\%}$	385 MPa	-0.7%
	$\sigma_{90\%}$	416 MPa	+0.1%

9. Figures

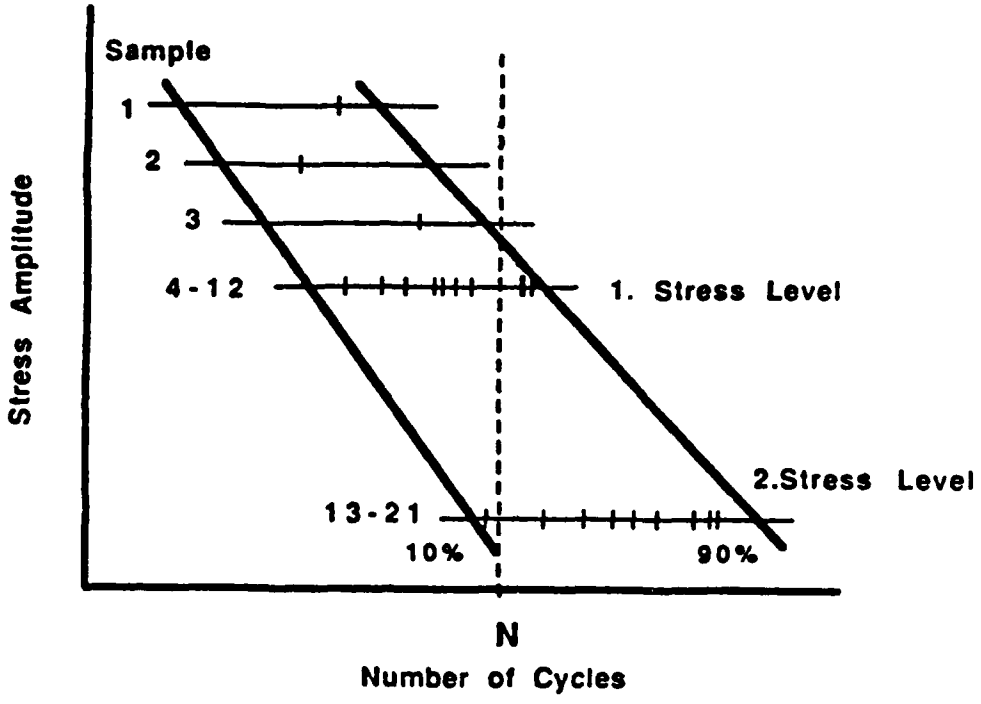

Figure 1: Procedure of the boundary technique in the range of finite endurance

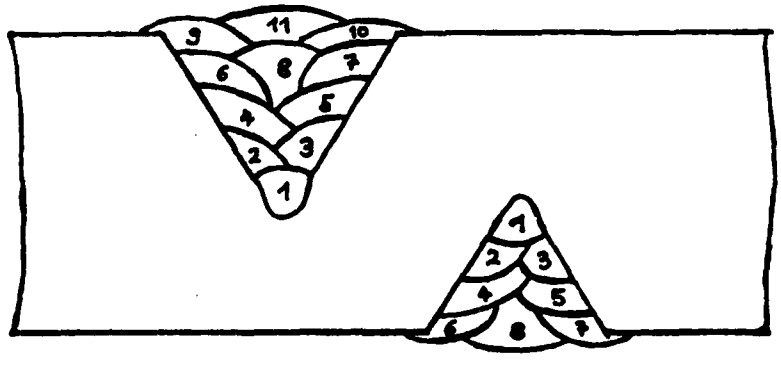

Figure 2: Pass sequence

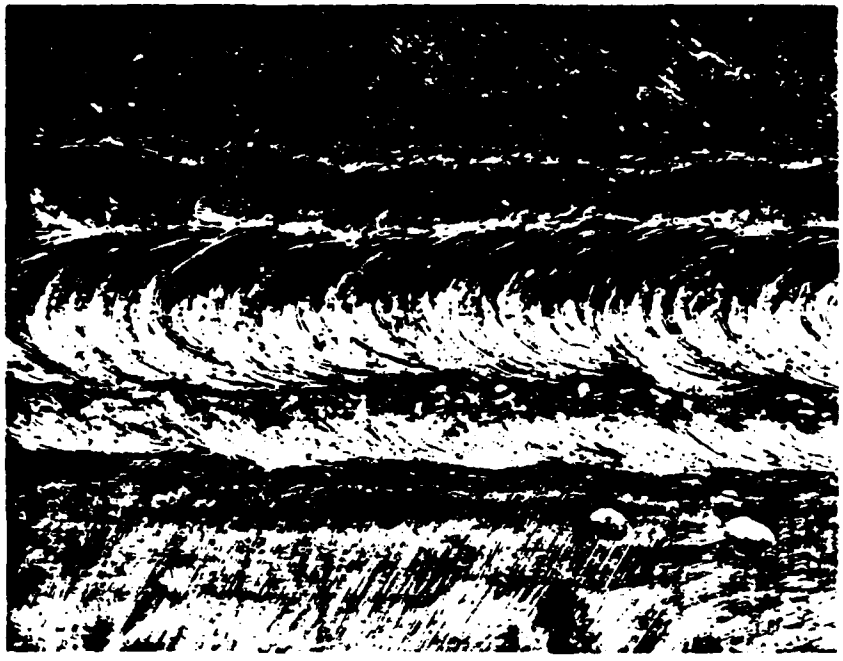

Figure 3: Typical weldment in plate 1 (2 x)

Figure 4: Typical weldment in plate 3 (2 x)

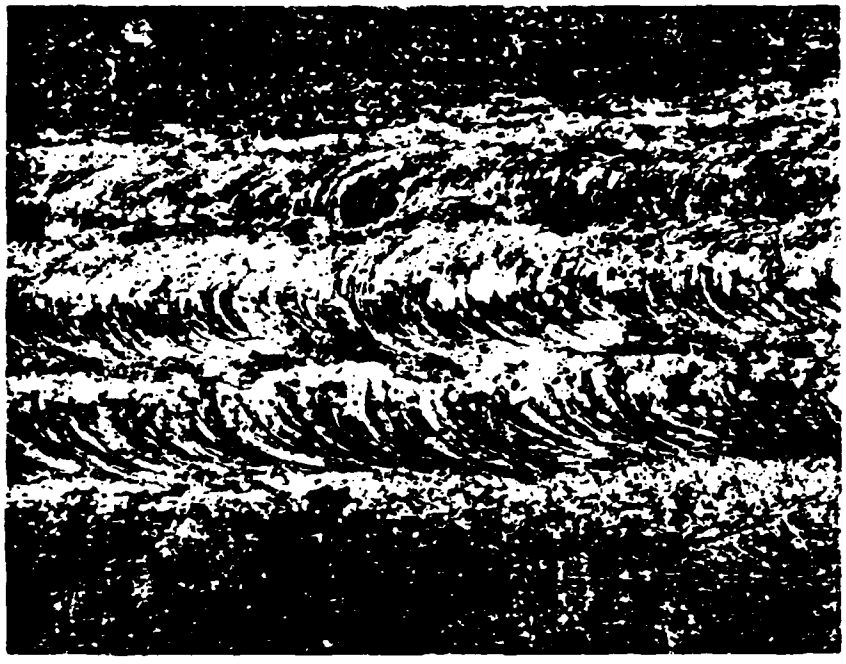

Figure 5: Typical weldment in plate 5 (2 x)

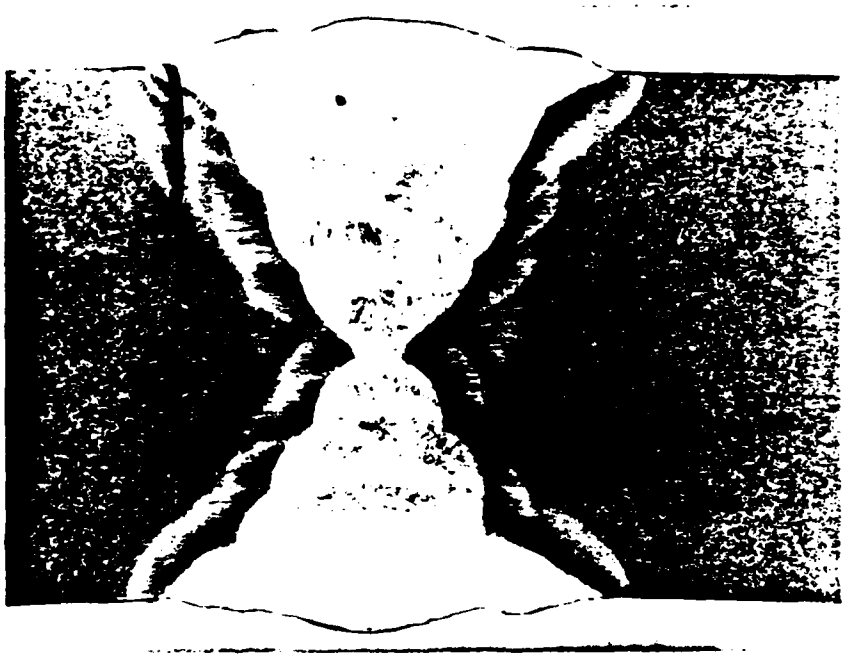

Figure 6: Cross section of the weldment in plate 1 with a crack at the top (2.5 x)

Figure 7: Cross section of the weldment in plate 3 with cracks at the top (2.5 x)

Figure 8: Cross section of the weldment in plate 5 (2.5 x)

Figure 9: Typical microstucture of the HAZ (right) and weld metal (left) (500 x)

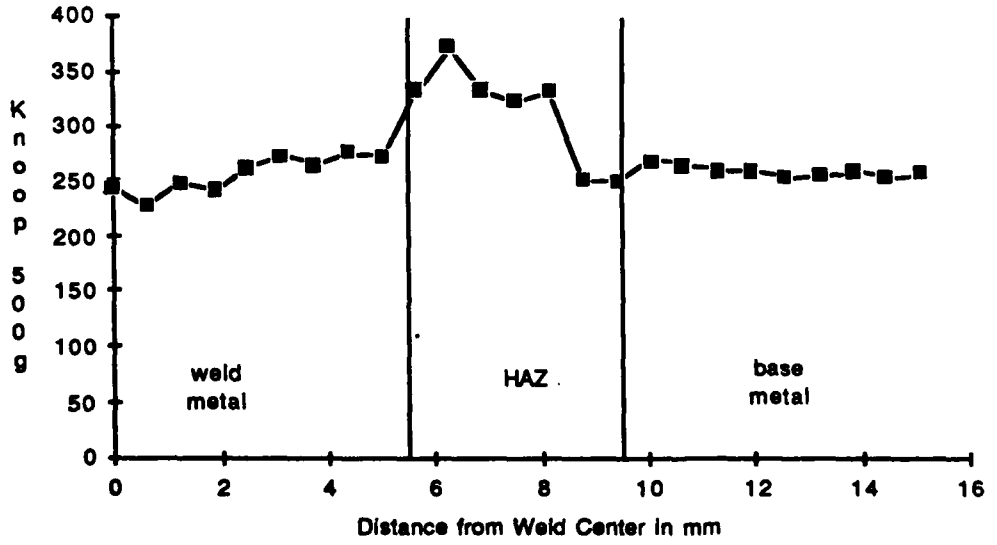

Figure 10: Microhardness across the weldment in plate 1

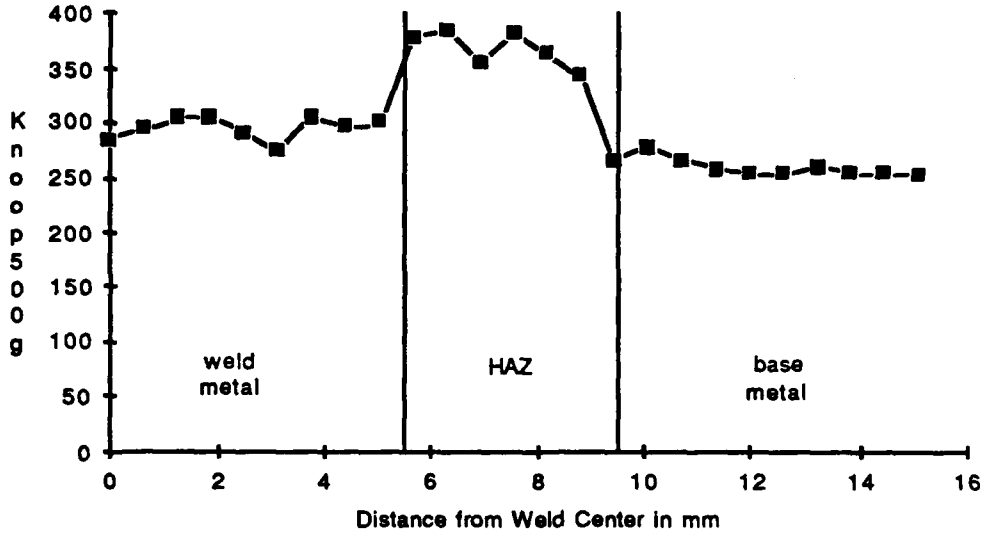

Figure 11: Microhardness across the weldment in plate 3

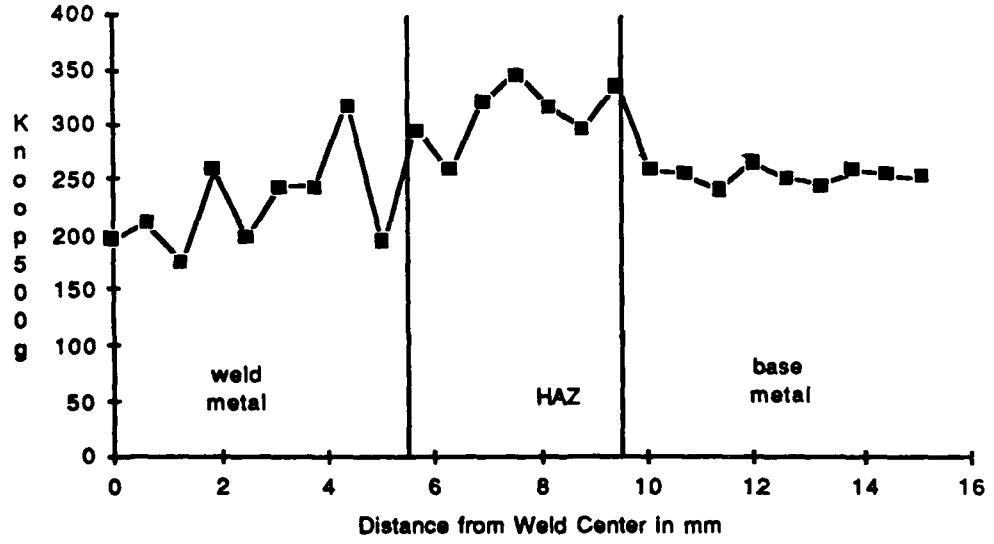

Figure 12: Microhardness across the weldment in plate 5

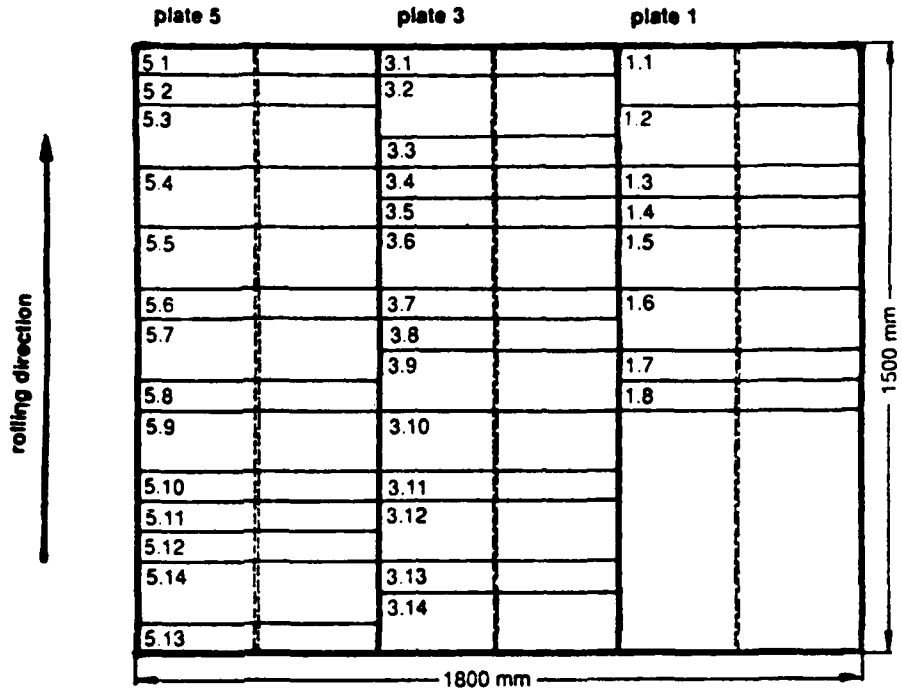

Figure 13: Sampling plan

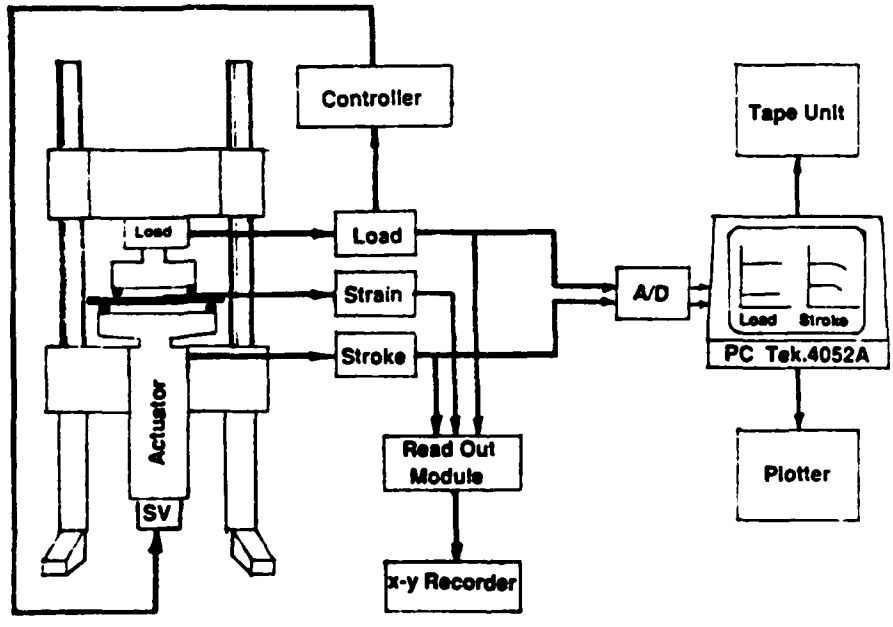

Figure 14: Test set-up for 4-point-bending fatigue test

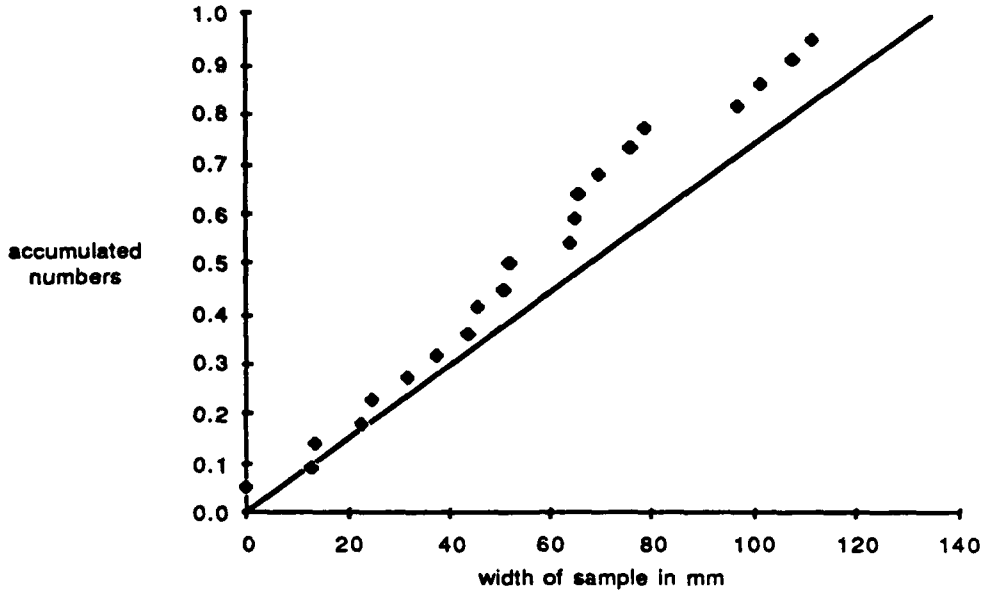

Figure 15: Distribution of the crack initiation points over the width of the unwelded samples

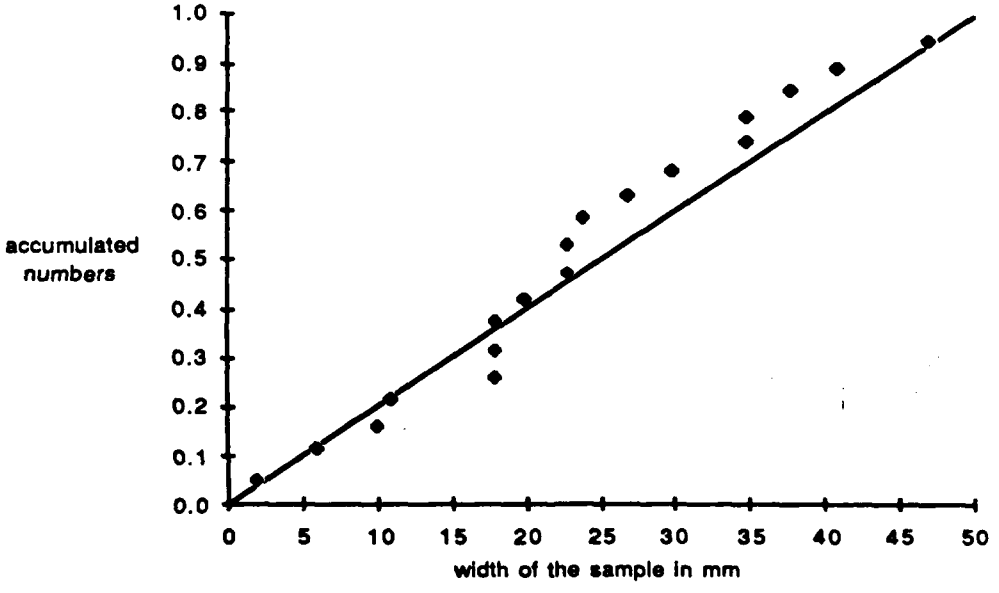

Figure 16: Distribution of the crack initiation points over the width of the 75 mm wide samples

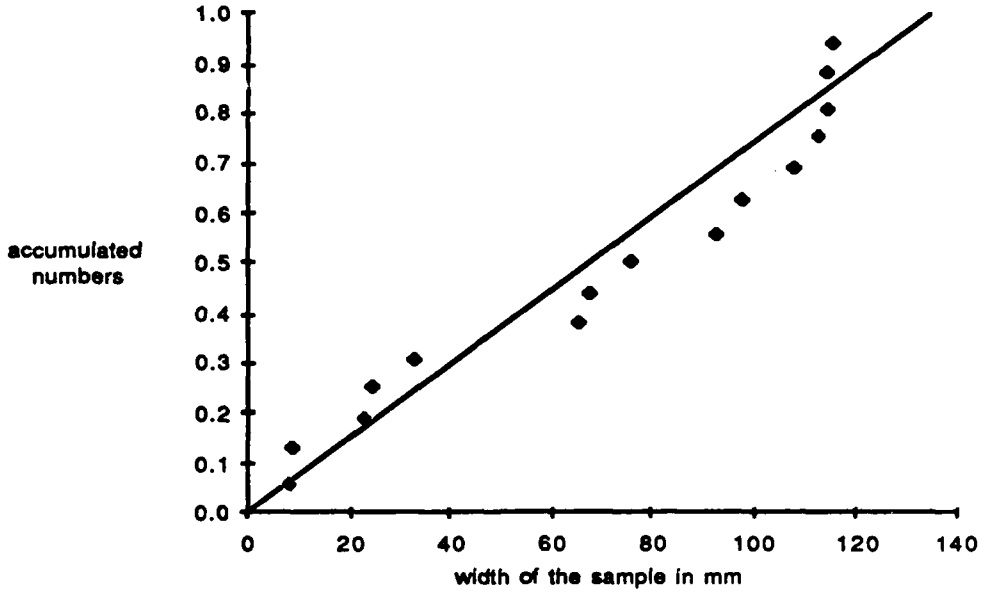

Figure 17: Distribution of the crack initiation points over the width of the 150 mm wide samples

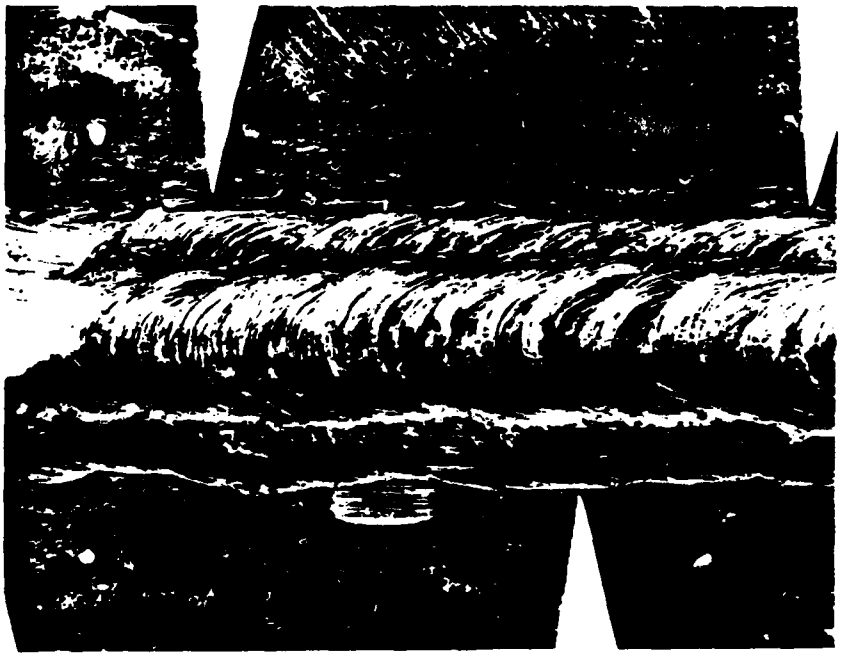

Figure 18: Weldment with several initial fatigue cracks on both sides of the weld metal (2 x)

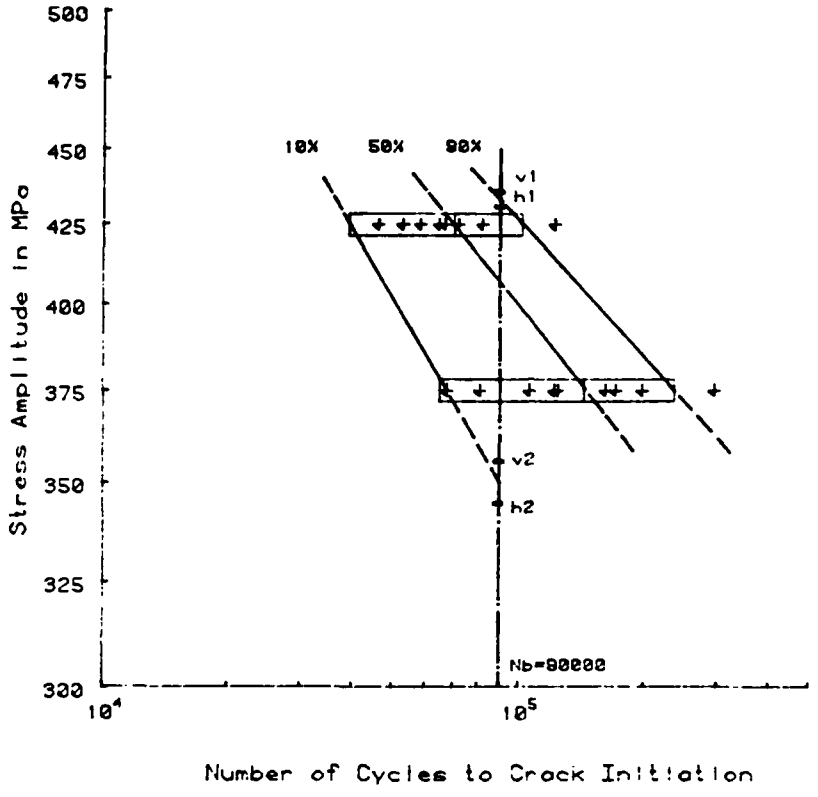

Figure 19: Wöhler-curve of the 75 mm wide samples

h_1, h_2 = horizontal analysis

v_1, v_2 = vertical analysis

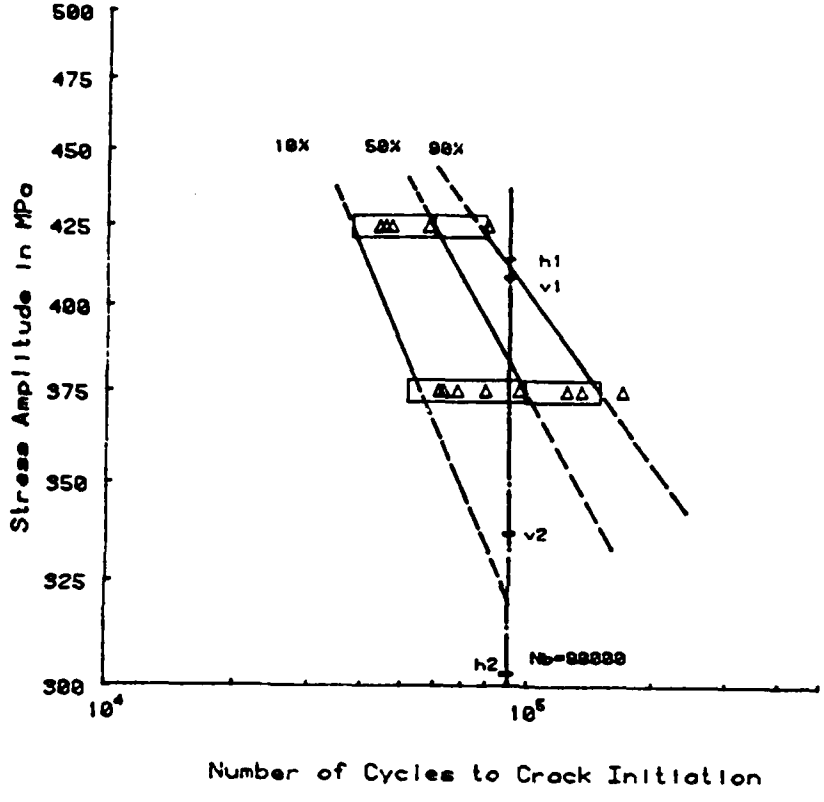

Figure 20: Wöhler-curve of the 150 mm wide samples

h_1, h_2 = horizontal analysis

v_1, v_2 = vertical analysis

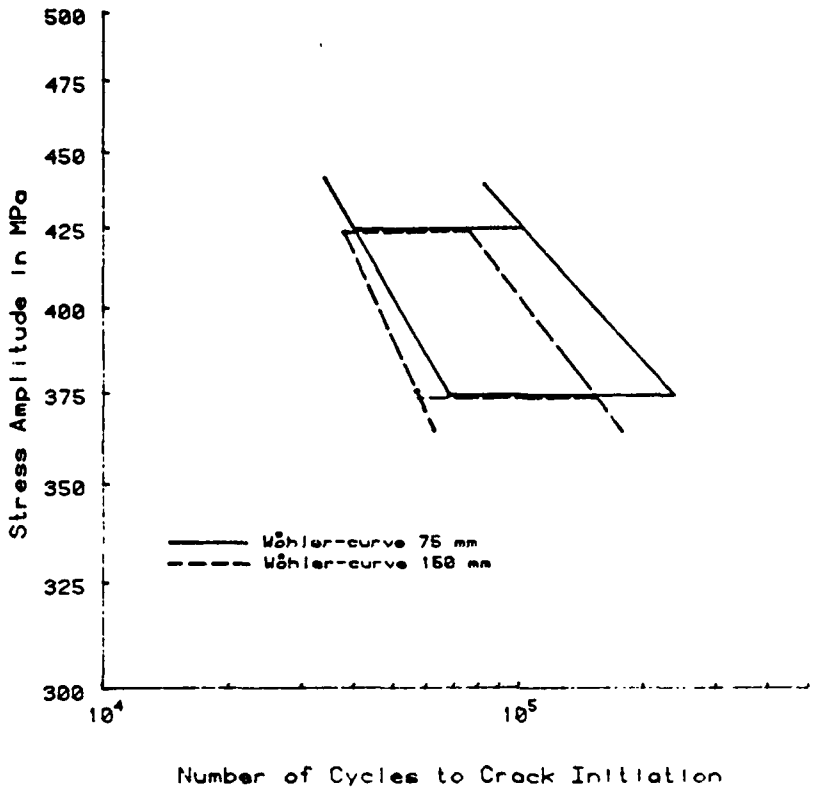

Figure 21: Comparision between the Wöhler-curves of 75mm and 150 mm wide samples

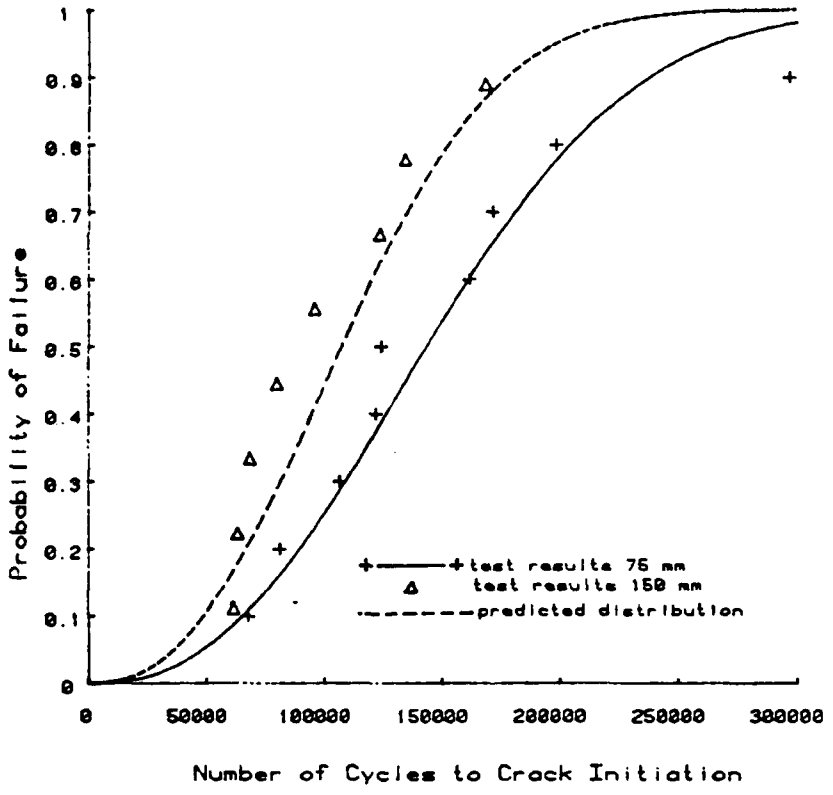

Figure 22: Prediction of the number of cycles to crack initiation of the 150 mm wide samples tested at the 375 MPa-stress level

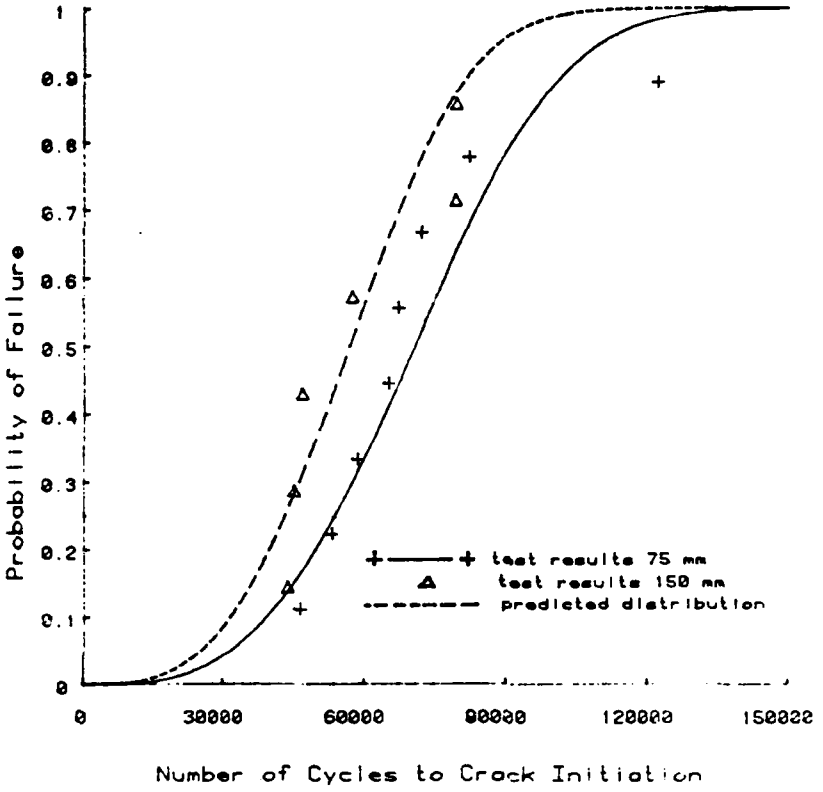

Figure 23: Prediction of the number of cycles to crack initiation of the 150 mm wide samples tested at the 425 MPa-stress level

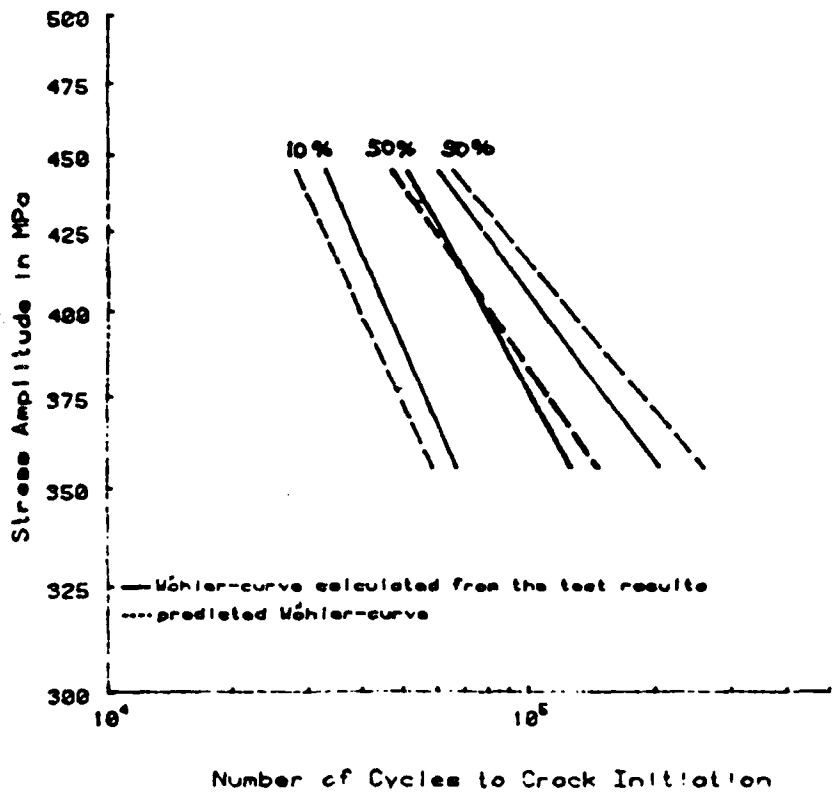

Figure 24: Comparision between the predicted Wöhler-curve and the test results (lines for a probability of failure of 10%, 50% and 90%)

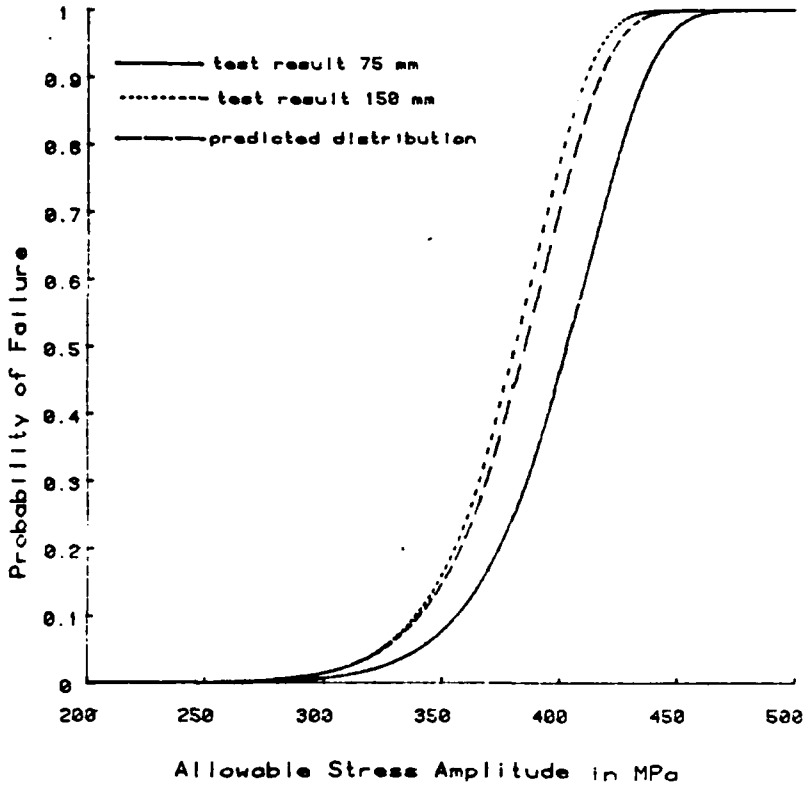

Figure 25: Prediction of the allowable stress amplitudes of the 150 mm wide samples at 90000 cycles

Figure 26: Typical fracture surface of a sample tested at the 375 MPa-stress level

Figure 27: Typical fracture surface of a sample tested at the 425 MPa-stress level

Appendix

Recordings of Test Results

DREA

Dockyard Lab

DETERMINATION OF CRACK-INITIATION

Plate 5.3/150mm
Stress min max
145, 520 MPa
Mat. : HY 100
Elec.: E12018M2
Pos. : flat

W. Kreuzer
28. July 1987

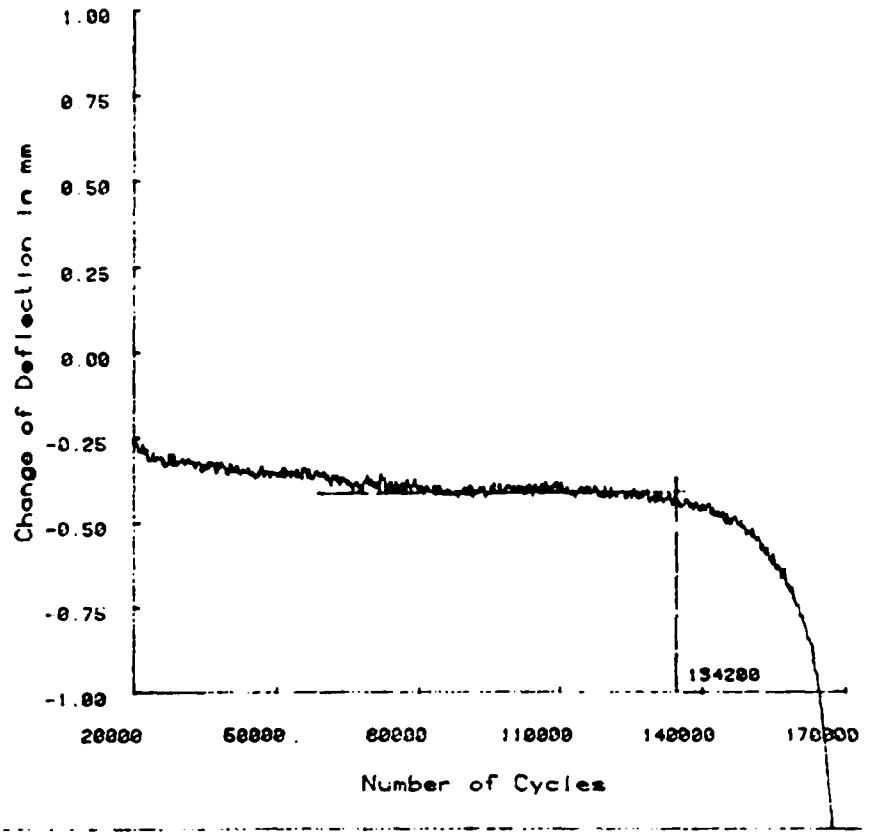

DREA

Dockyard Lab

DETERMINATION OF CRACK-INITIATION

Plate 5.13/150mm
Stress min max
145, 520 MPa
Mat. : HY 100
Elec.: E12018M2
Pos. : flat

W. Kreuzer
22. July 1987

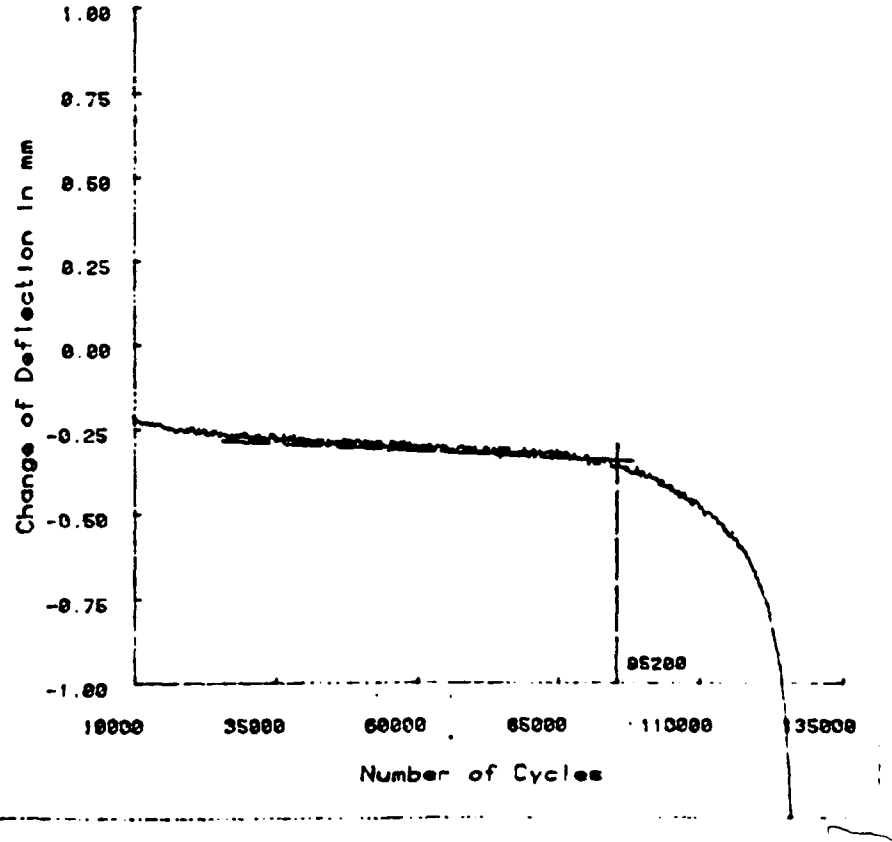

DREA

Dockyard Lab

DETERMINATION

OF CRACK-

INITIATION

Plate 3.3/75mm
Stress min max
185, 650 MPa
Mat. : HY 100
Elec.: E12018M2
Pos. : flat

W. Kreuzer
24. June 1987

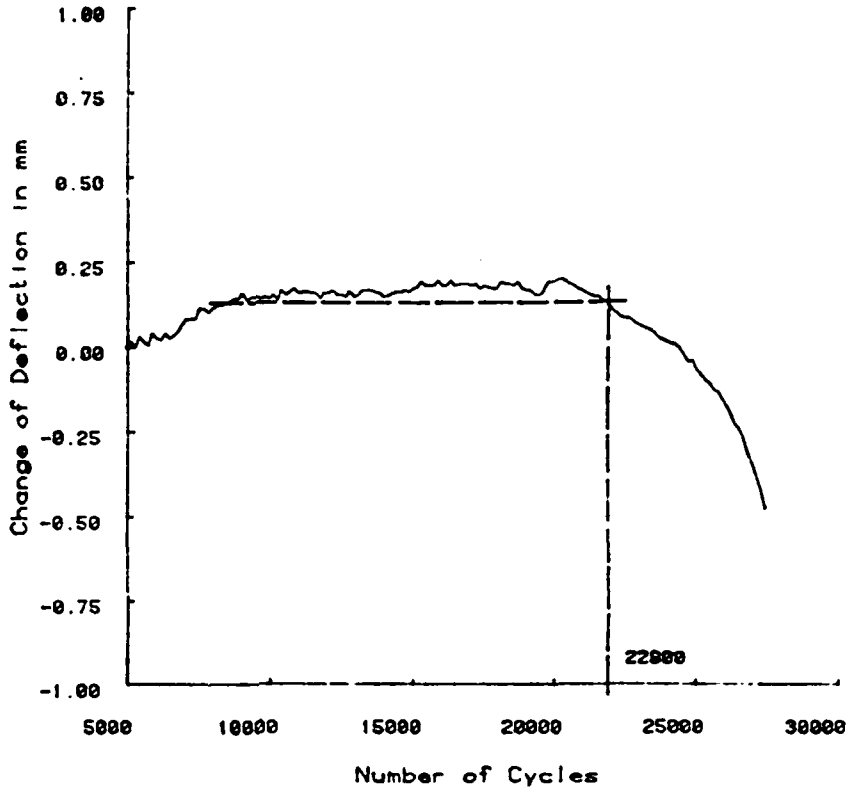

DREA

Dockyard Lab

DETERMINATION

OF CRACK-

INITIATION

Plate 5.12/75mm
Stress min max
180, 620 MPa
Mat. : HY 100
Elec.: E12018M2
Pos. : flat

W. Kreuzer
24. June 1987

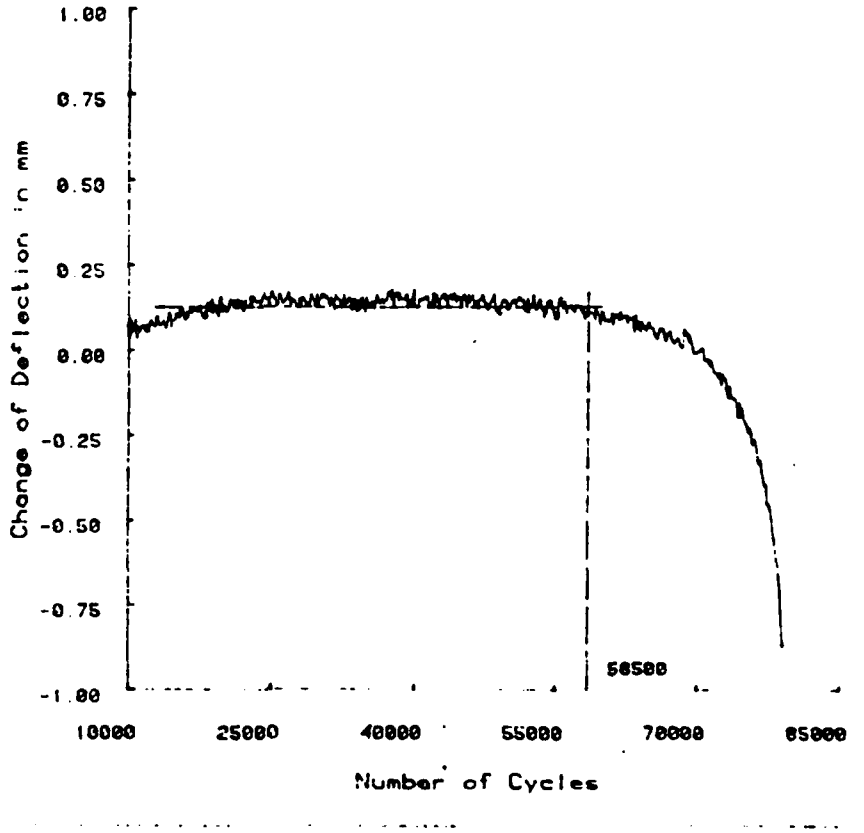

DREA

Dockyard Lab

DETERMINATION

OF CRACK-

INITIATION

Plate 1.4/75mm
Stress min max
165, 590 MPa
Mat. : HY 100
Elec.: E12018M2
Pos. : flat

W. Kreuzer
24. June 1987

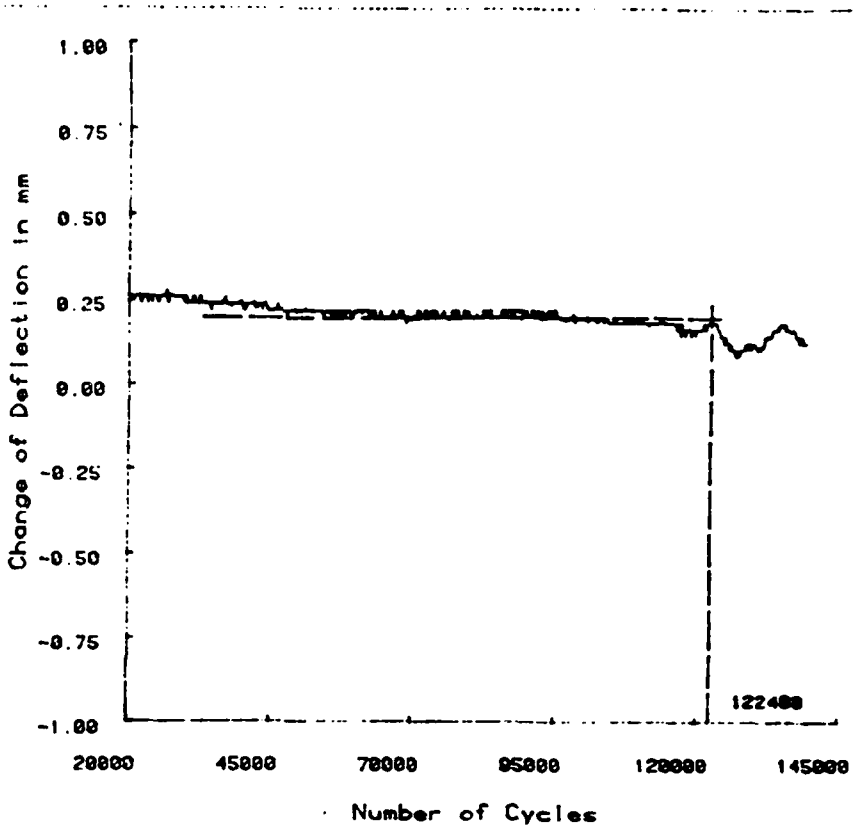

DREA

Dockyard Lab

DETERMINATION

OF CRACK-

INITIATION

Plate 1.7/75mm
Stress min max
165, 590 MPa
Mat. : HY 100
Elec.: E12018M2
Pos. : flat

W. Kreuzer
6. July 1987

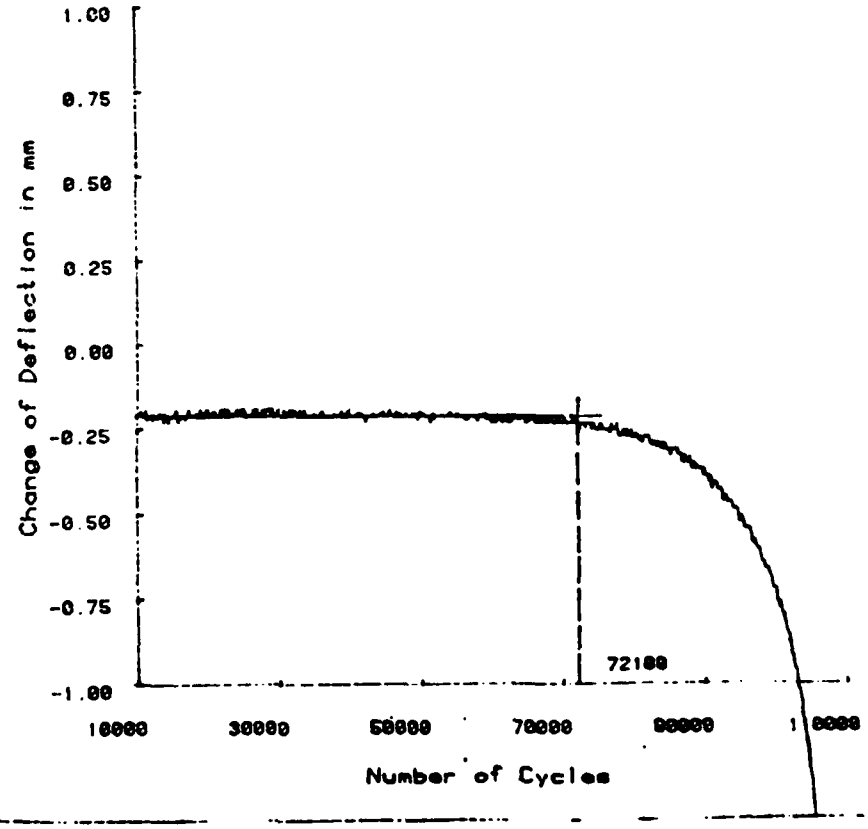

DREA

Dockyard Lab

DETERMINATION OF CRACK-INITIATION

Plate 3.4/75mm
Stress min max
165, 590 MPa
Mat. : HY 100
Elec.: E12018M2
Pos. : flat

W. Kreuzer
24. June 1987

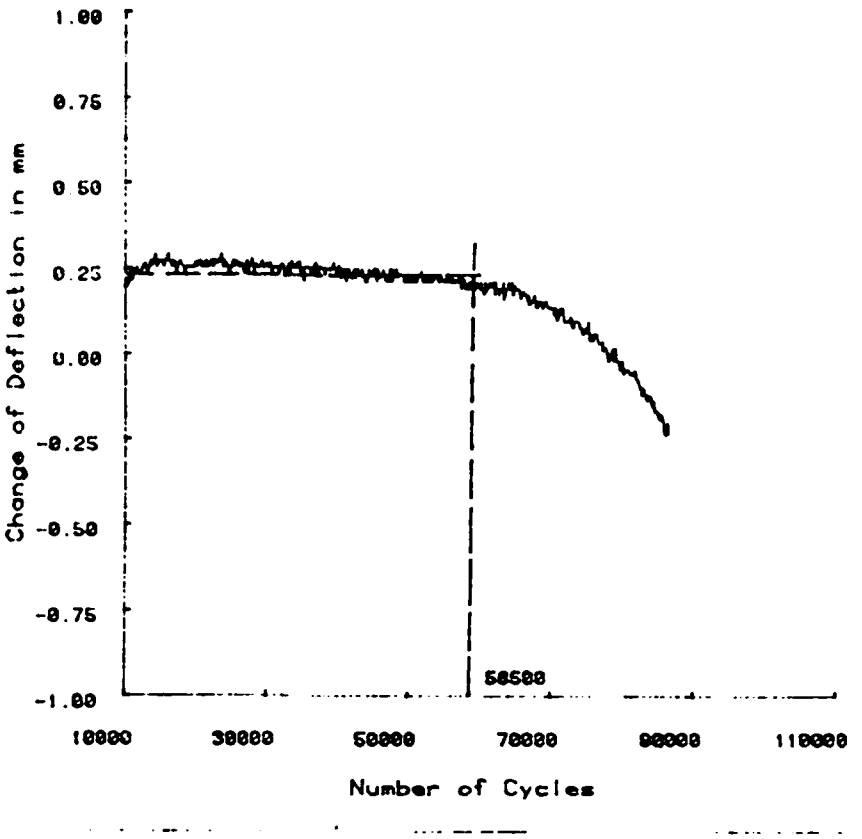

DREA

Dockyard Lab

DETERMINATION OF CRACK-INITIATION

Plate 3.5/75mm
Stress min max
165, 590 MPa
Mat. : HY 100
Elec.: E12018M2
Pos. : flat

W. Kreuzer
24. June 1987

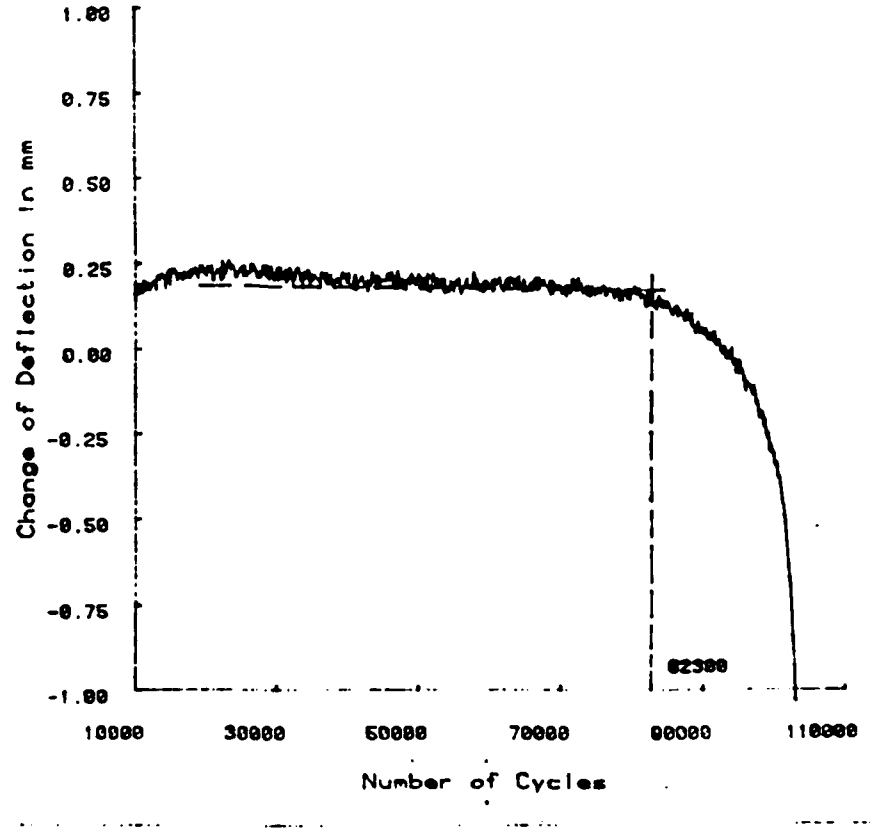

DREA

Dockyard Lab

DETERMINATION OF CRACK-INITIATION

Plate 3.8/75mm
Stress min max
165, 590 MPa
Mat. : HY 100
Elec.: E12018M2
Pos. : flat

W. Kreuzer
7. July 1987

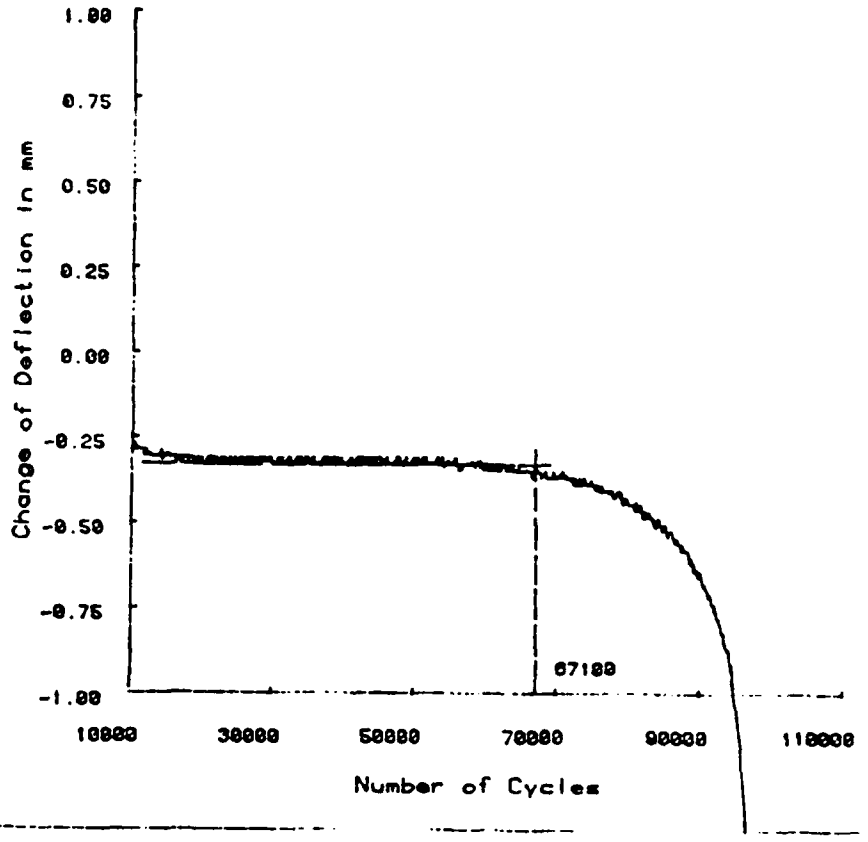

DREA

Dockyard Lab

DETERMINATION OF CRACK-INITIATION

Plate 5.1/75mm
Stress min max
165, 590 MPa
Mat : HY 100
Elec.: E12018M2
Pos. : flat

W. Kreuzer
6 July 1987

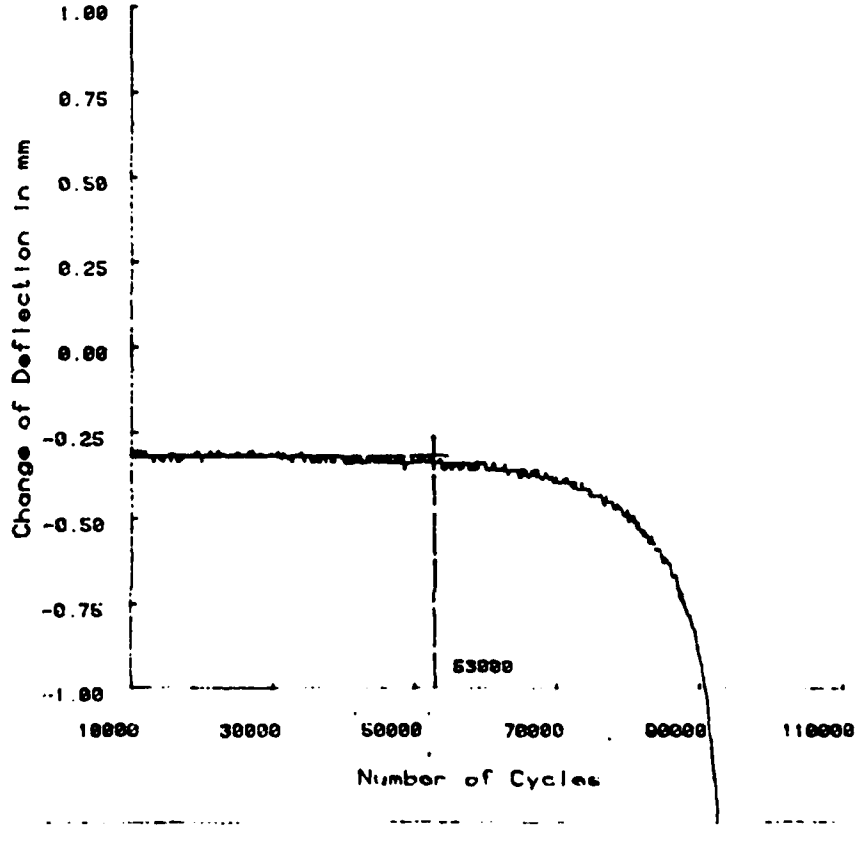

DREA

Dockyard Lab

DETERMINATION

OF CRACK-

INITIATION

Plate 5.11/75mm
Stress min max
165, 590 MPa
Mat. : HY 100
Elec.: E12018M2
Pos. : flat

W. Kreuzer
24. June 1987

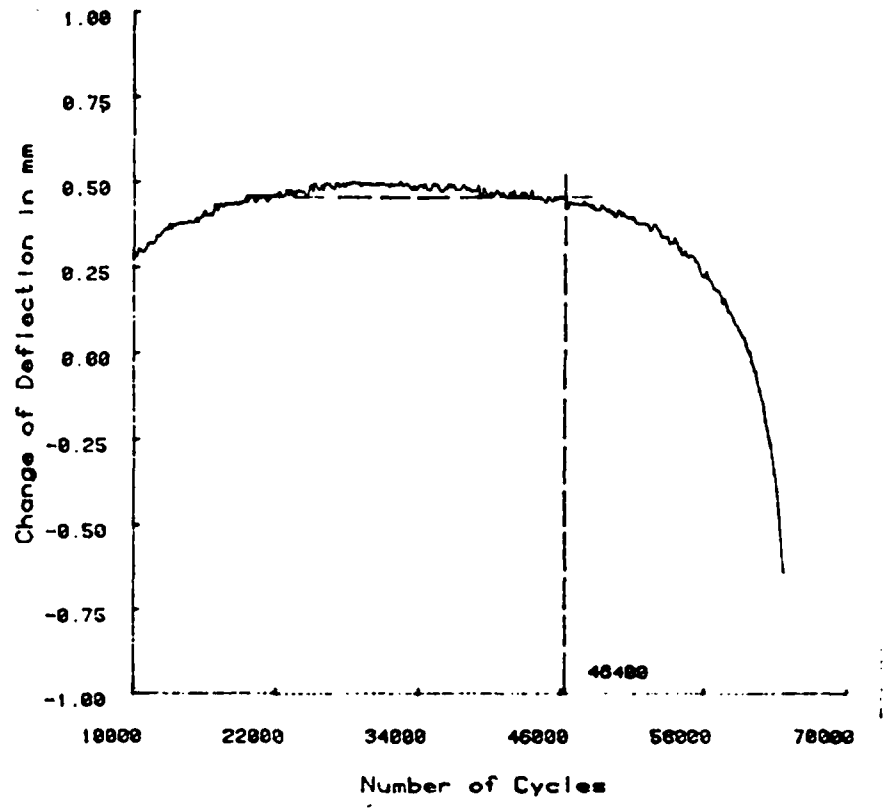

DREA

Dockyard Lab

DETERMINATION

OF CRACK-

INITIATION

Plate 5.14/75mm
Stress min max
165, 590 MPa
Mat. : HY 100
Elec.: E12018M2
Pos. : flat

W. Kreuzer
6. July 1987

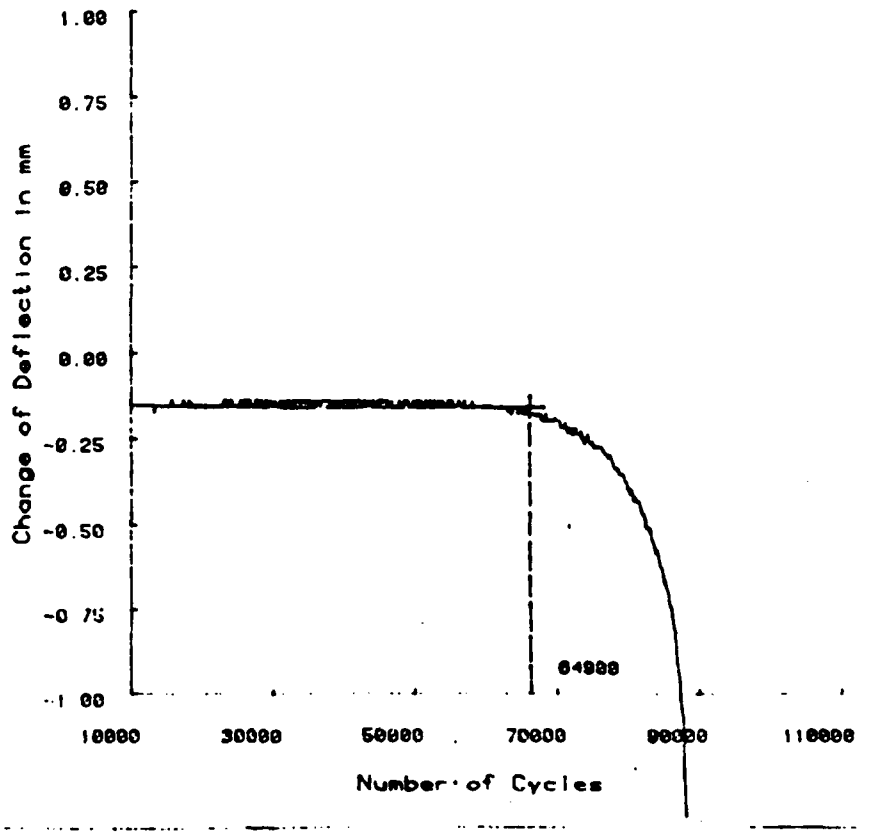

DREA

Dockyard Lab

DETERMINATION OF CRACK-INITIATION

Plate 1.8/75mm
Stress min max
145, 520 MPa
Mat. : HY 100
Elec.: E12018M2
Pos. : flat

W. Kreuzer
14. July 1987

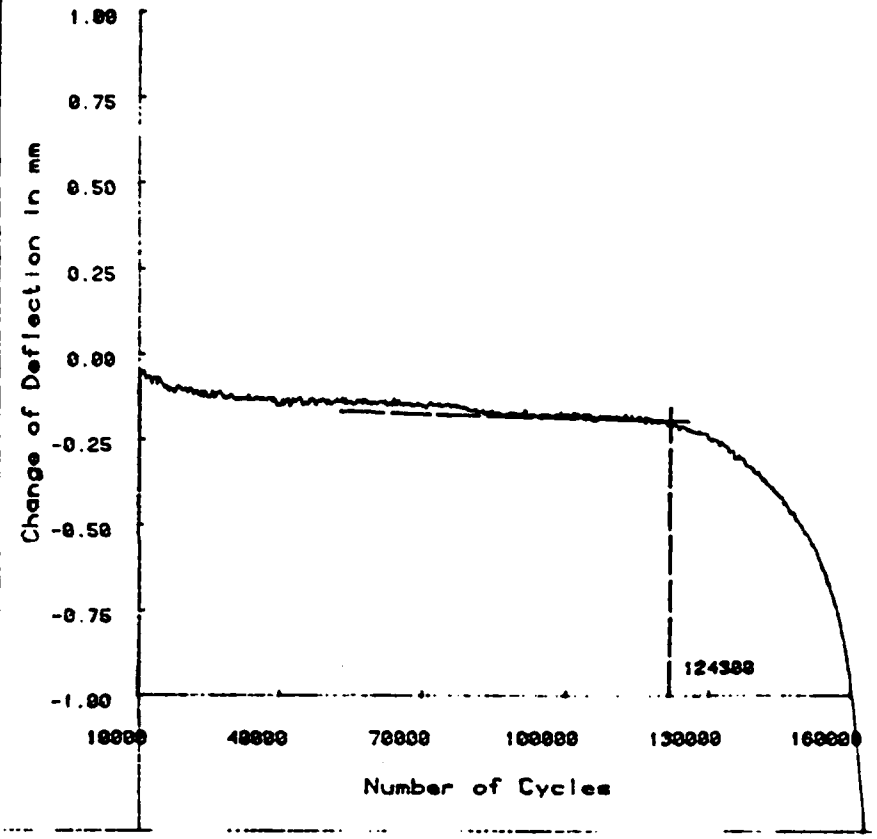

DREA

Dockyard Lab

DETERMINATION OF CRACK-INITIATION

Plate 3.1/75mm
Stress min max
145, 520 MPa
Mat. : HY 100
Elec.: E12018M2
Pos. : flat

W. Kreuzer
16. July 1987

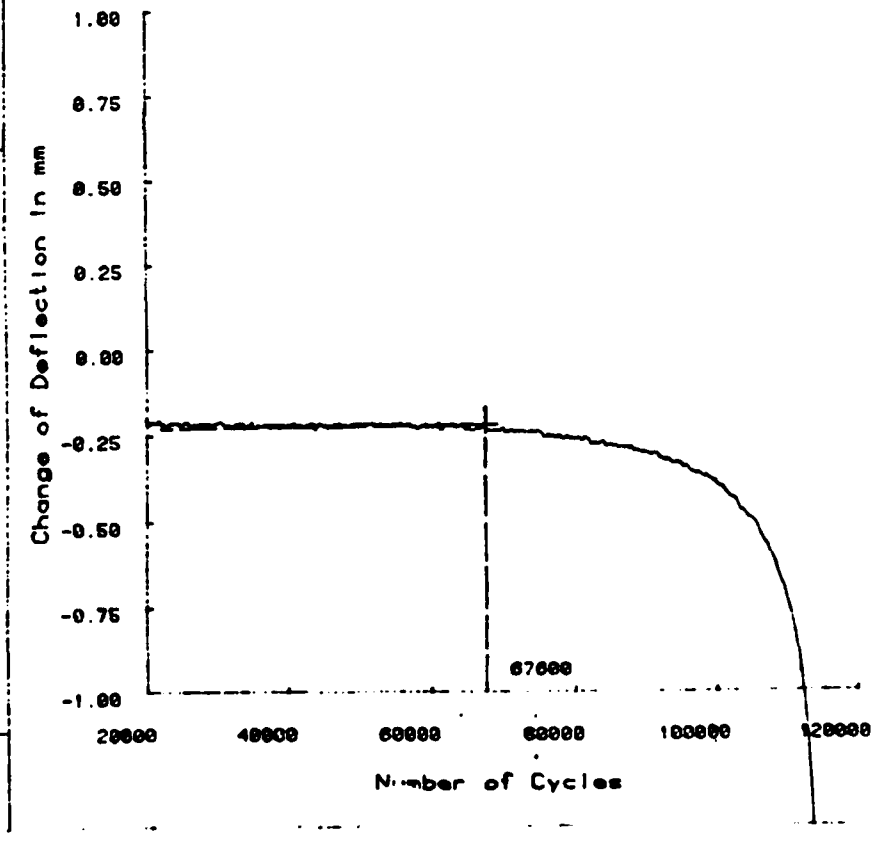

DREA

Dockyard Lab

DETERMINATION OF CRACK-INITIATION

Plate 3 II /75mm
Stress min max
145, 520 MPa
Mat. : HY 100
Elec.: E12018M2
Pos. : flat

W. Kreuzer
10. July 1987

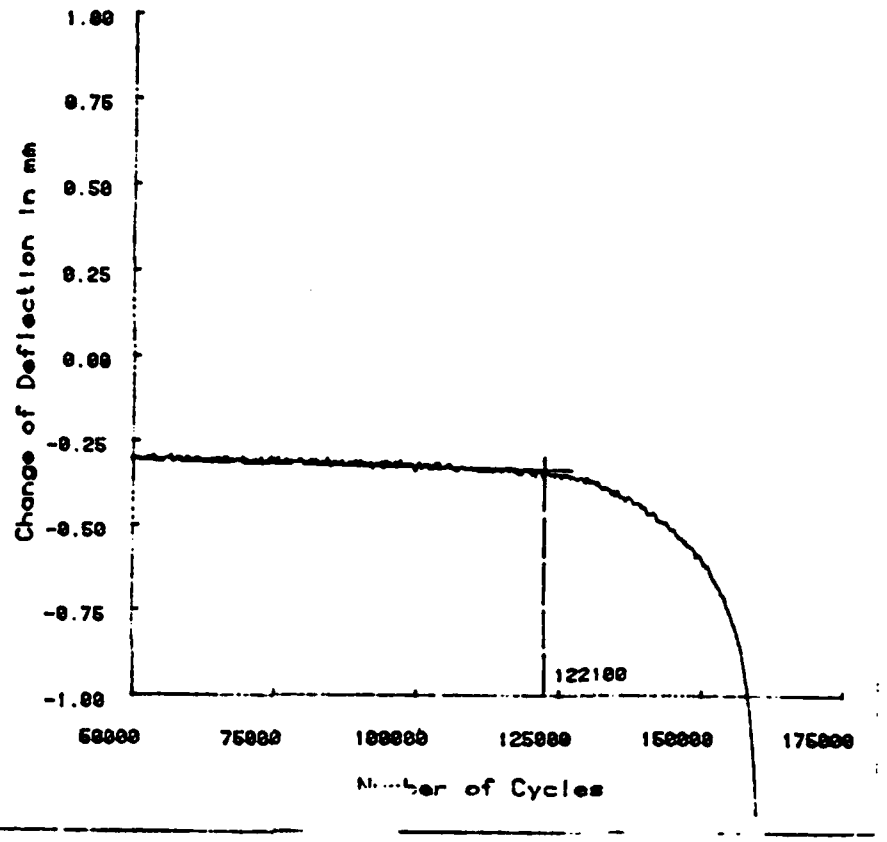

DREA

Dockyard Lab

DETERMINATION OF CRACK-INITIATION

Plate 3.13/75mm
Stress min max
145, 520 MPa
Mat. : HY 100
Elec.: E12018M2
Pos. : flat

W. Kreuzer
15. July 1987

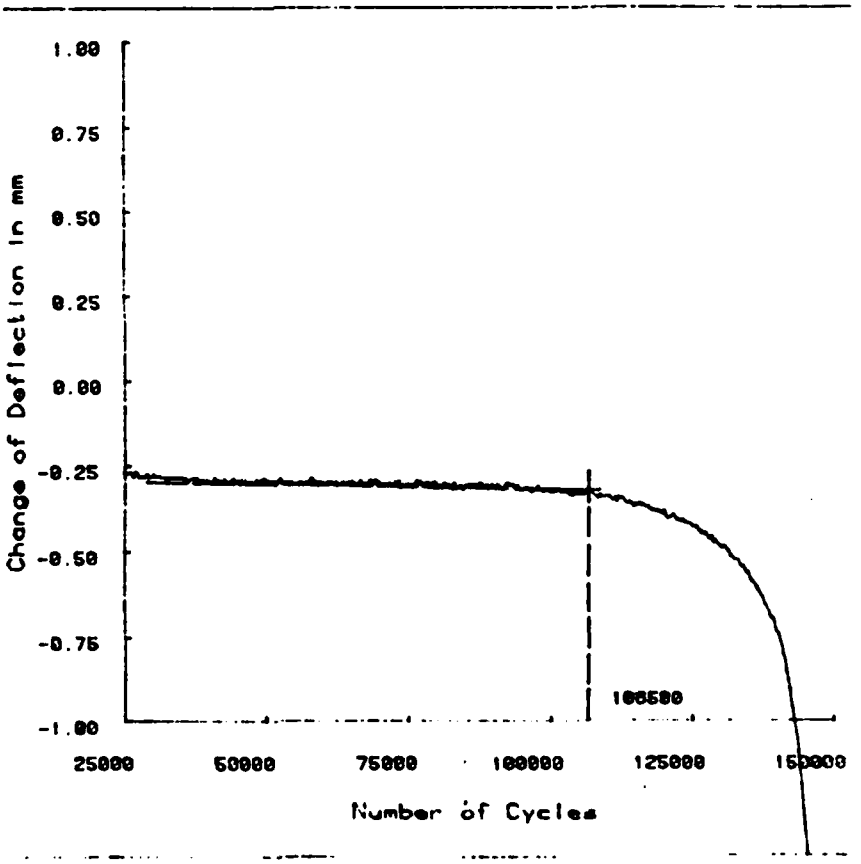

DREA

Dockyard Lab

DETERMINATION

OF CRACK-

INITIATION

Plate 5.1/75mm
Stress min max
145, 520 MPa
Mat. : HY 100
Elec.: E12018M2
Pos. : flat

W. Kreuzer
18. July 1987

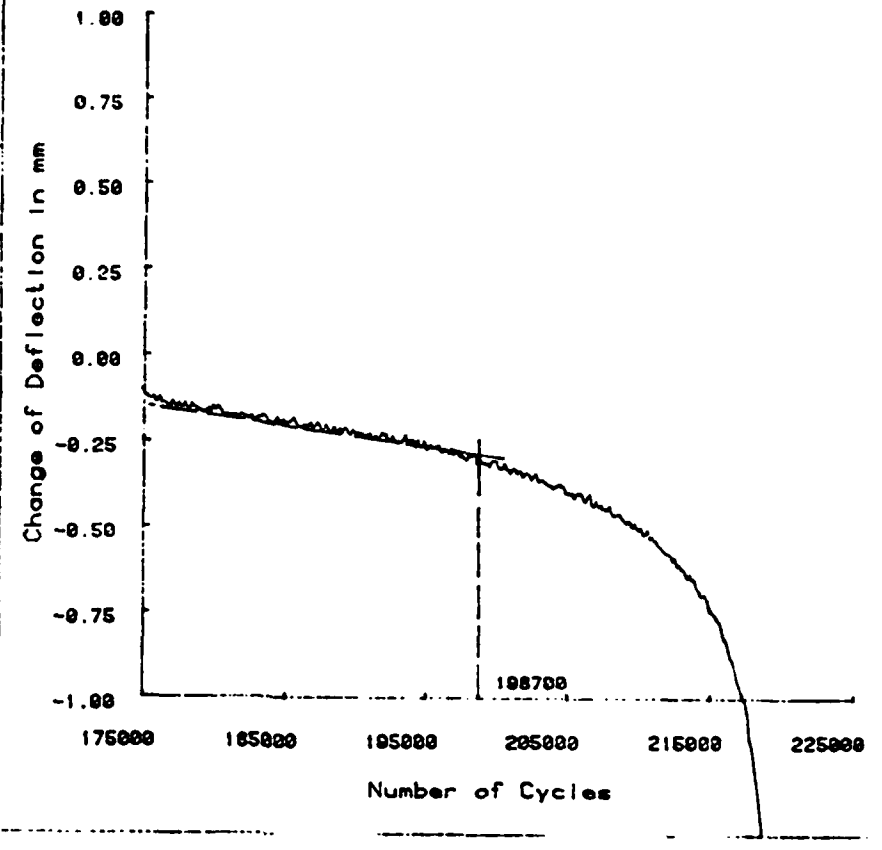

DREA

Dockyard Lab

DETERMINATION

OF CRACK-

INITIATION

Plate 5.2/75mm
Stress min max
145, 520 MPa
Mat. : HY 100
Elec.: E12018M2
Pos. : flat

W. Kreuzer
17. July 1987

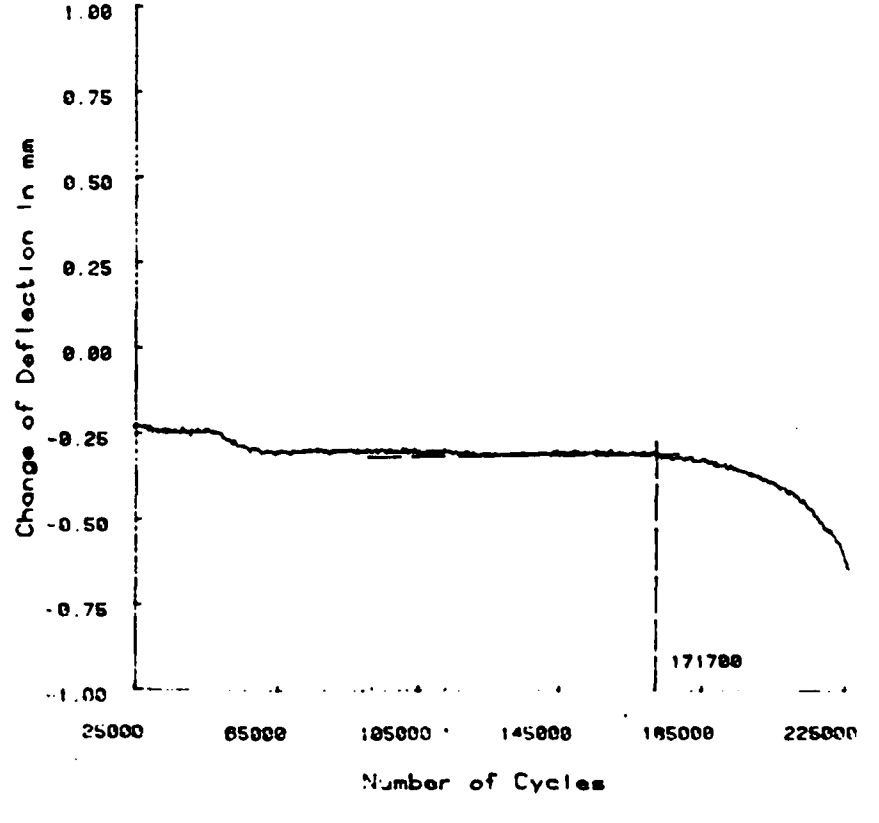

DREA

Dockyard Lab

DETERMINATION OF CRACK-INITIATION

Plate 1.6/150mm
Stress min max
165, 590 MPa
Mat. : HY 100
Elec.: E12018M2
Pos. : flat

W. Kreuzer
27. June 1987

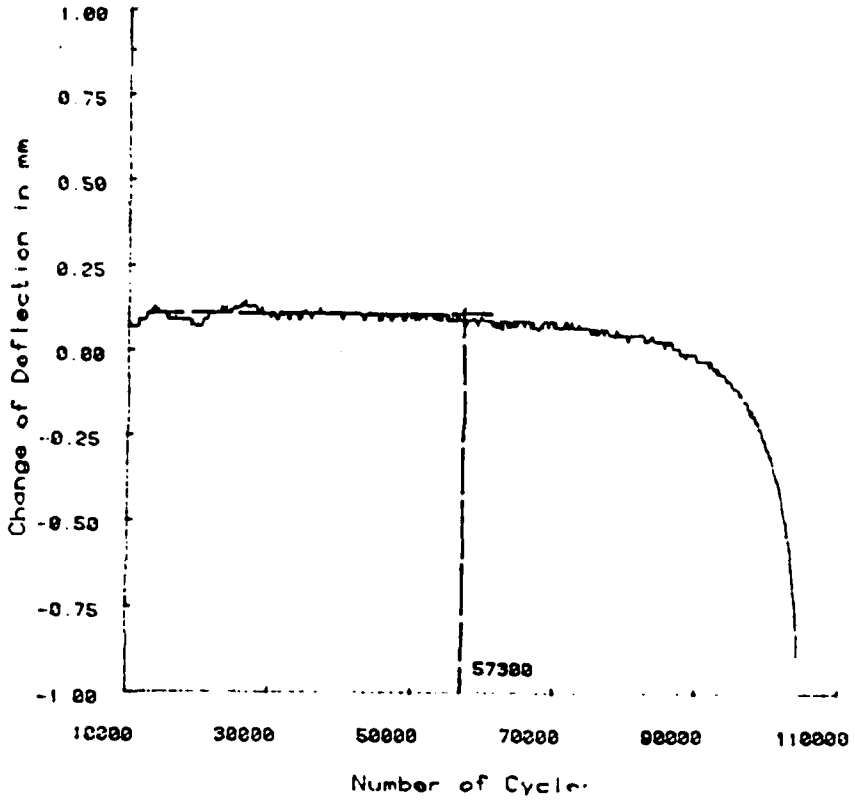

DREA

Dockyard Lab

DETERMINATION OF CRACK-INITIATION

Plate 3.6/150mm
Stress min max
165, 590 MPa
Mat. : HY 100
Elec.: E12018M2
Pos. : flat

W. Kreuzer
26. June 1987

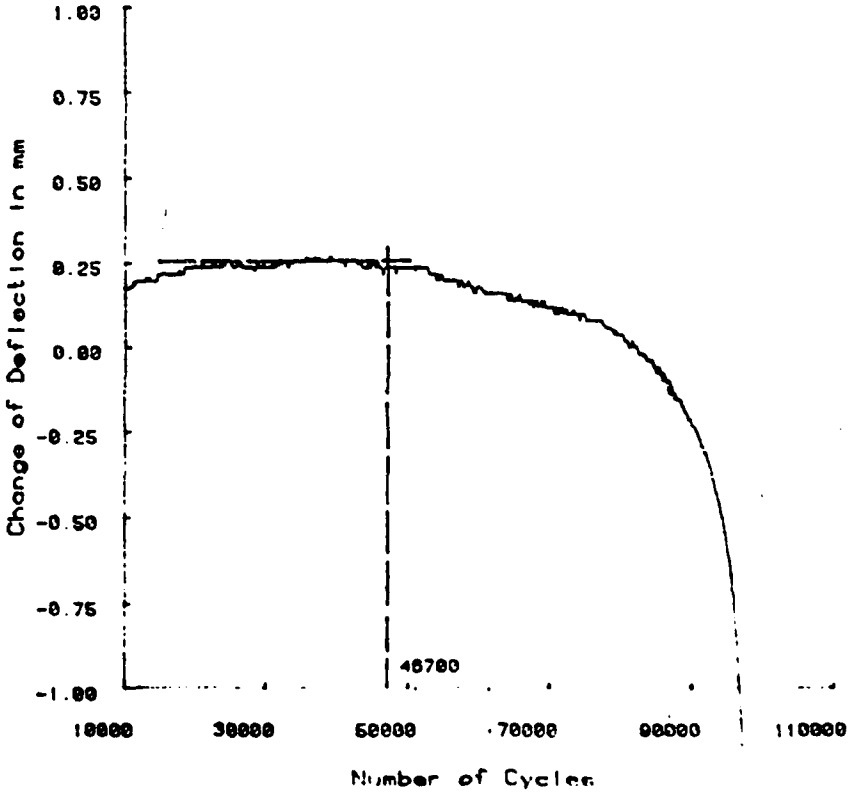

DREA

Dockyard Lab

DETERMINATION OF CRACK-INITIATION

Plate 3.1/150mm
Stress min max
165, 590 MPa
Mat. : HY 100
Elec.: E12018M2
Pos. : flat

W. Kreuzer
30. June 1987

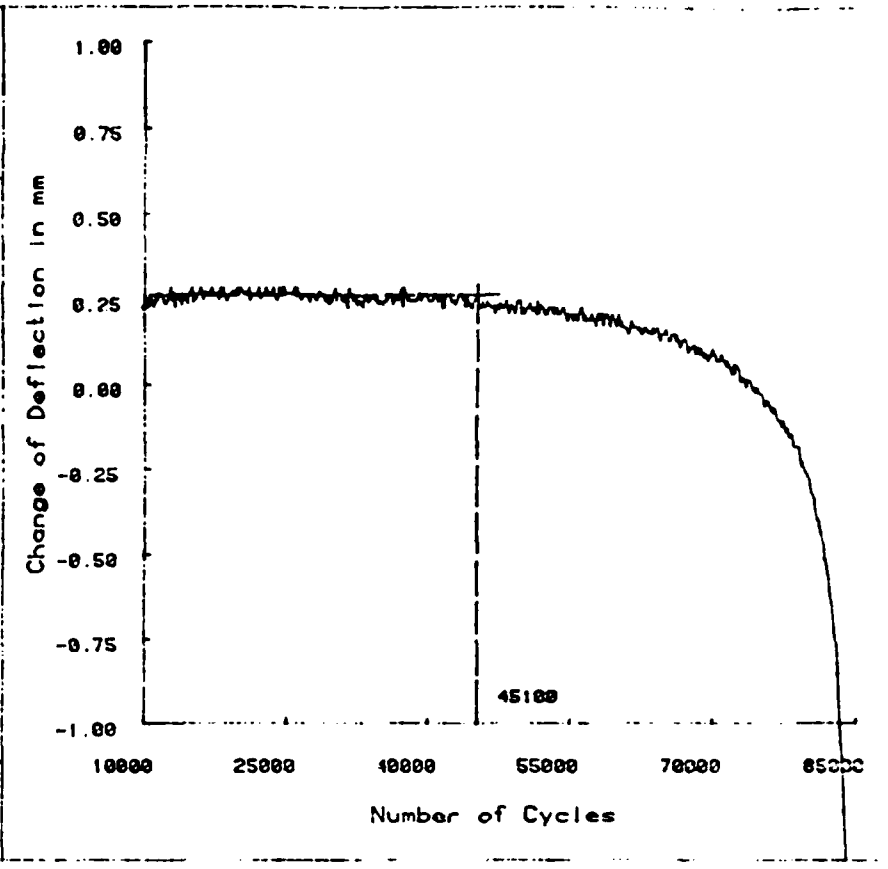

DREA

Dockyard Lab

DETERMINATION OF CRACK-INITIATION

Plate 5.4/150mm
Stress min max
165, 590 MPa
Mat. : HY 100
Elec.: E12018M2
Pos. : flat

W. Kreuzer
23. JUNE 1987

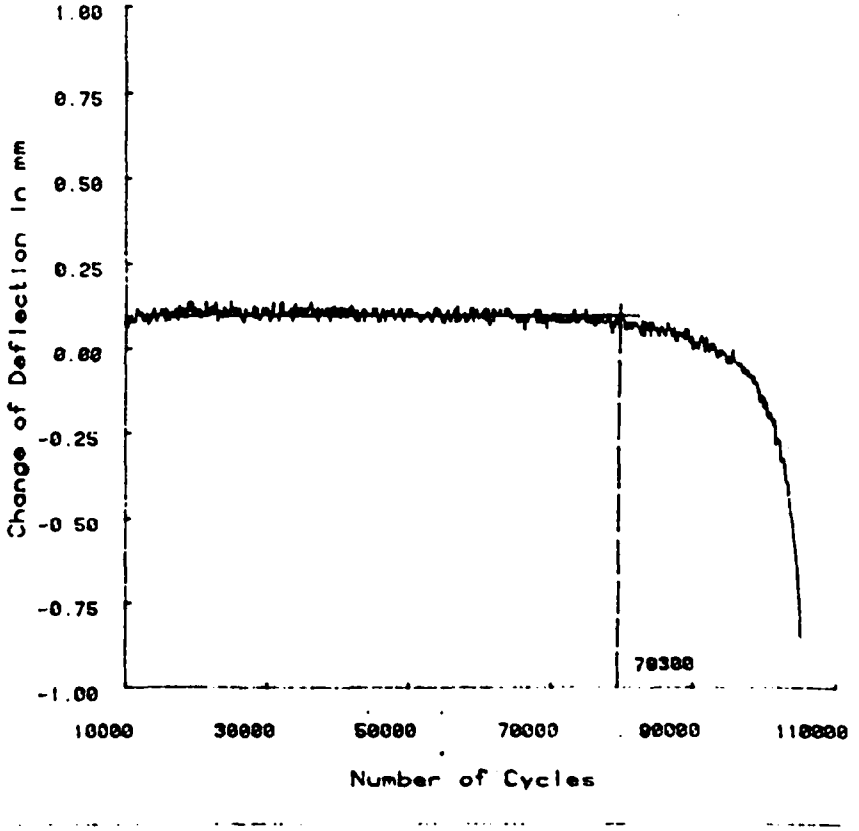

DREA

Dockyard Lab

DETERMINATION OF CRACK-INITIATION

Plate 5.5/150mm
Stress min max
165, 590 MPa
Mat. : HY 100
Elec.: E12018M2
Pos. : flat

W. Kreuzer
25. June 1987

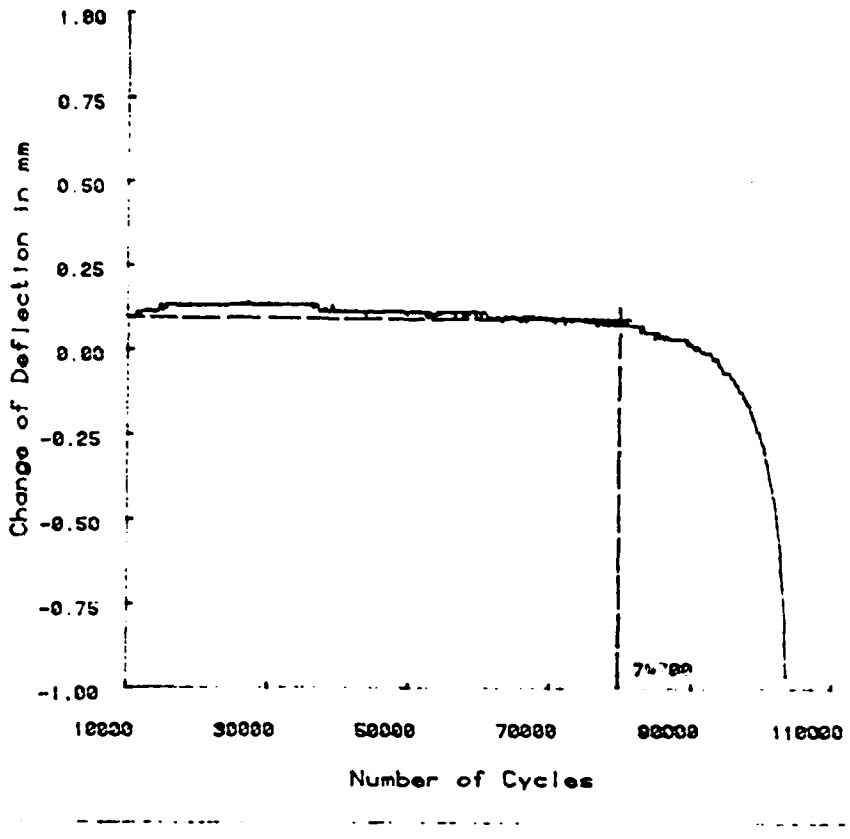

DREA

Dockyard Lab

DETERMINATION OF CRACK-INITIATION

Plate 5.9/150mm
Stress min max
165, 590 MPa
Mat. : HY 100
Elec.: E12018M2
Pos. : flat

W. Kreuzer
23. JUNE 1987

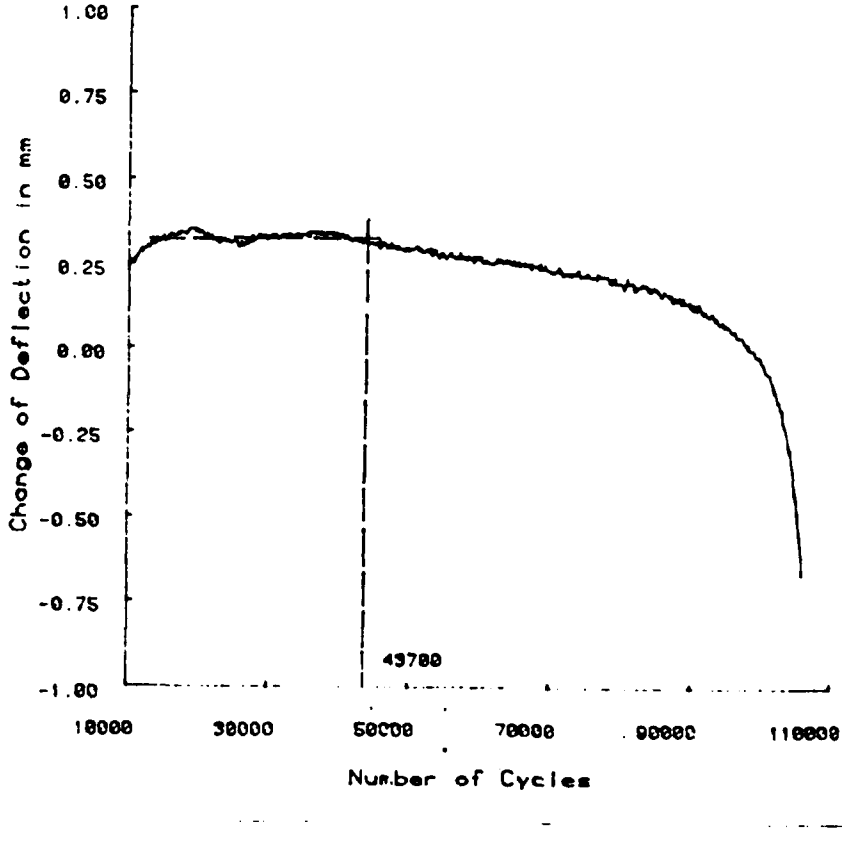

DREA

Dockyard Lab

DETERMINATION OF CRACK-INITIATION

Plate 1.1/150mm
Stress min max
145, 520 MPa
Mat. : HY 100
Elec.: E12018M2
Pos. : flat

W. Kreuzer
24. July 1987

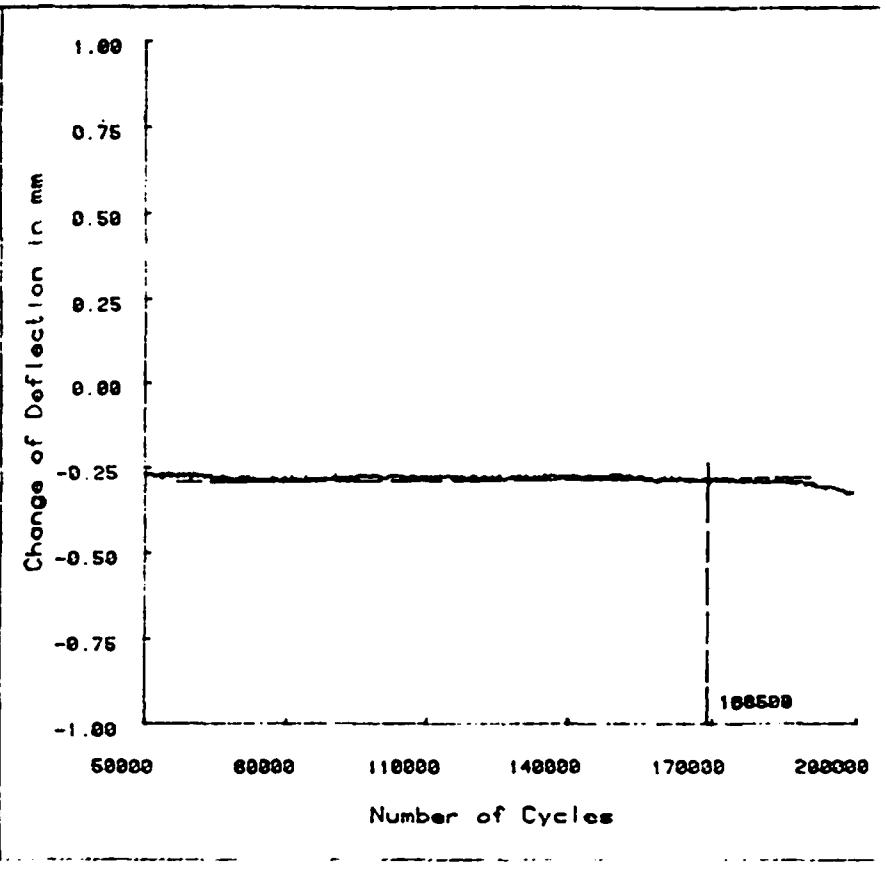

DREA

Dockyard Lab

DETERMINATION OF CRACK-INITIATION

Plate 3.2/150mm
Stress min max
145, 520 MPa
Mat. : HY 100
Elec.: E12018M2
Pos. : flat

W. Kreuzer
21. July 1987

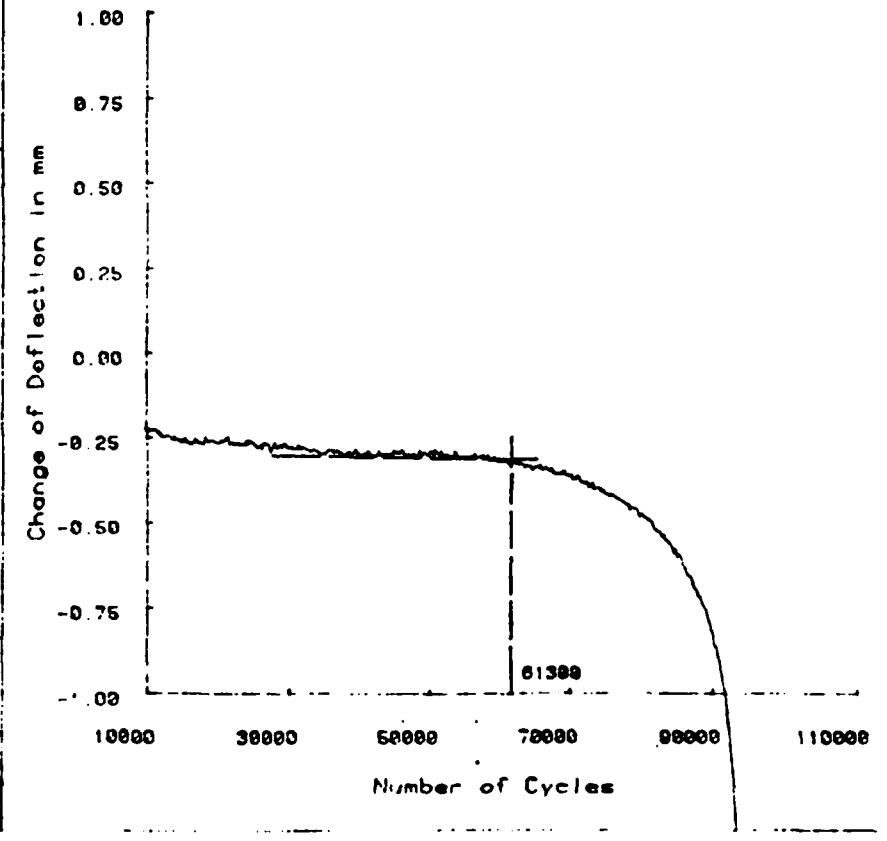

DREA

Dockyard Lab

DETERMINATION OF CRACK-INITIATION

Plate 3.9/150mm
Stress min max
145, 520 MPa
Mat. : HY 100
Elec.: E12018M2
Pos. : flat

W. Kreuzer
26. July 1987

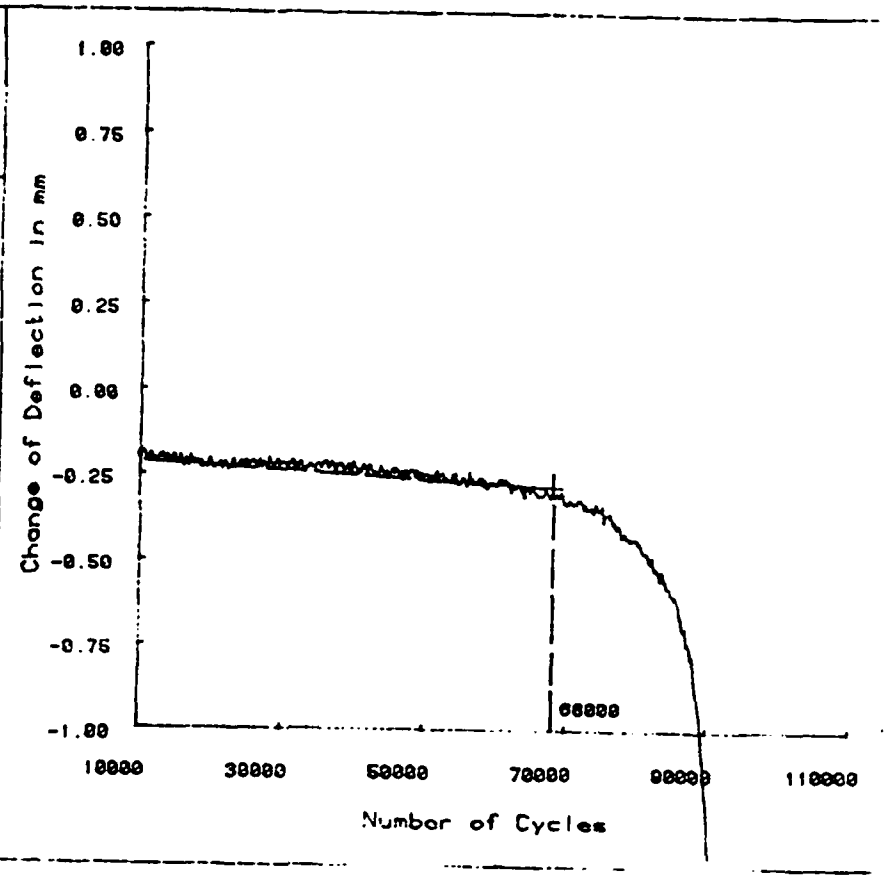

DREA

Dockyard Lab

DETERMINATION OF CRACK-INITIATION

Plate 3.12/150mm
Stress min max
145, 520 MPa
Mat. : HY 100
Elec.: E12018M2
Pos. : flat

W. Kreuzer
23. July 1987

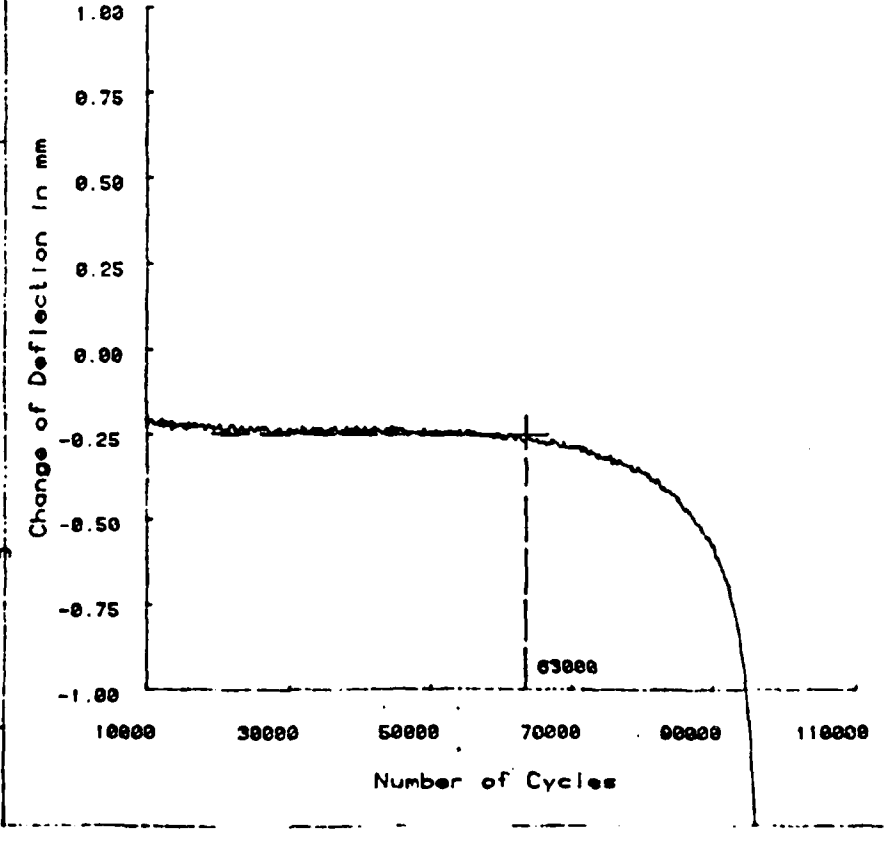

DREA

Dockyard Lab

DETERMINATION

OF CRACK-

INITIATION

Plate 3.14/150mm
Stress min max
145, 520 MPa
Mat. : HY 100
Elec.: E12018M2
Pos. : flat

W. Kreuzer
20. July 1987

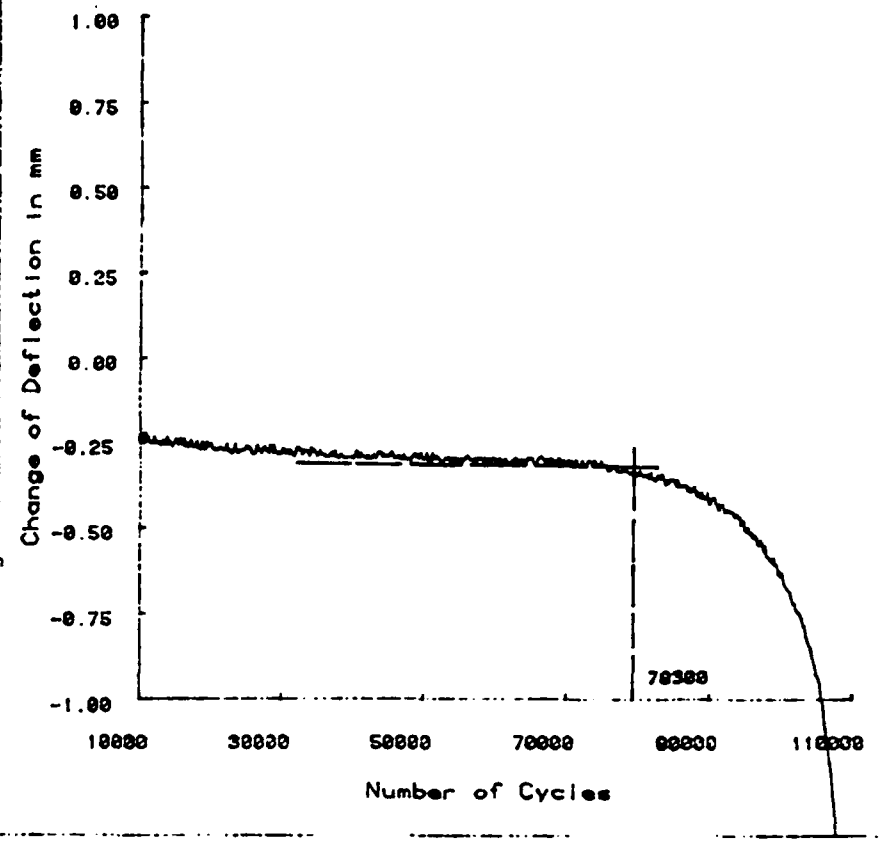

UNCLASSIFIED

SECURITY CLASSIFICATION OF FORM
(highest classification of Title, Abstract, Keywords)

DOCUMENT CONTROL DATA

(Security classification of title, body of abstract and indexing annotation must be entered when the overall document is classified)

1. ORIGINATOR (the name and address of the organization preparing the document. Organizations for whom the document was prepared, e.g. Establishment sponsoring a contractor's report, or tasking agency, are entered in section 8.)

Defence Research Establishment Atlantic
P.O. Box 1012, Dartmouth, N.S. B2Y 3Z7

2. SECURITY CLASSIFICATION (overall security classification of the document, including special warning terms if applicable)

UNCLASSIFIED

3. TITLE (the complete document title as indicated on the title page. Its classification should be indicated by the appropriate abbreviation (S,C,R or U) in parentheses after the title.)

INFLUENCE OF SPECIMEN SIZE ON FATIGUE CRACK INITIATION OF WELDED HY100 STEEL

4. AUTHORS (Last name, first name, middle initial. If military, show rank, e.g. Doe, Maj. John E.)

Kreuzer, Wolfgang A.

5. DATE OF PUBLICATION (month and year of publication of document)	6a. NO. OF PAGES (total containing information. Include Annexes, Appendices, etc.)	6b. NO. OF REFS (total cited in document)
JANUARY 1988	72	12

6. DESCRIPTIVE NOTES (the category of the document, e.g. technical report, technical note or memorandum. If appropriate, enter the type of report, e.g. interim, progress, summary, annual or final. Give the inclusive dates when a specific reporting period is covered.)

Technical Memorandum

8. SPONSORING ACTIVITY (the name of the department project office or laboratory sponsoring the research and development. Include the address.)

Defence Research Establishment Atlantic, P.O. Box 1012, Dartmouth, N.S. B2Y 3Z7

9a. PROJECT OR GRANT NO. (If appropriate, the applicable research and development project or grant number under which the document was written. Please specify whether project or grant)	9b. CONTRACT NO. (If appropriate, the applicable number under which the document was written)

10a. ORIGINATOR'S DOCUMENT NUMBER (the official document number by which the document is identified by the originating activity. This number must be unique to this document.)	10b. OTHER DOCUMENT NOS. (Any other numbers which may be assigned this document either by the originator or by the sponsor)
DREA TECHNICAL MEMORANDUM 88/201	

11. DOCUMENT AVAILABILITY (any limitations on further dissemination of the document, other than those imposed by security classification)

(XX) Unlimited distribution
( ) Distribution limited to defence departments and defence contractors; further distribution only as approved
( ) Distribution limited to defence departments and Canadian defence contractors; further distribution only as approved
( ) Distribution limited to government departments and agencies; further distribution only as approved
( ) Distribution limited to defence departments; further distribution only as approved
( ) Other (please specify):

12. DOCUMENT ANNOUNCEMENT (any limitation to the bibliographic announcement of this document. This will normally correspond to the Document Availability (11). However, where further distribution (beyond the audience specified in 11) is possible, a wider announcement audience may be selected.)

UNCLASSIFIED

SECURITY CLASSIFICATION OF FORM

13. ABSTRACT (a brief and factual summary of the document. It may also appear elsewhere in the body of the document itself. It is highly desirable that the abstract of classified documents be unclassified. Each paragraph of the abstract shall begin with an indication of the security classification of the information in the paragraph (unless the document itself is unclassified) represented as (S), (C), (R), or (U). It is not necessary to include here abstracts in both official languages unless the text is bilingual).

The assumption of a statistical distribution of the flaws in a component leads to a prediction of a correlation between crack initiation life and the size of a fatigue loaded part. The influence of the specimen size on the fatigue crack initiation behaviour was analyzed for two series of welded HY100 steel plates of different widths. The weldments were prepared with E12018M2 electrodes.

The applicability of the theory of the statistical size effect was shown in the range of finite endurance. The prediction of the number of cycles to crack initiation and of the allowable stresses for samples of a different size agreed well with the experimental results.

14. KEYWORDS, DESCRIPTORS or IDENTIFIERS (technically meaningful terms or short phrases that characterize a document and could be helpful in cataloguing the document. They should be selected so that no security classification is required. Identifiers, such as equipment model designation, trade name, military project code name, geographic location may also be included. If possible keywords should be selected from a published thesaurus, e.g. Thesaurus of Engineering and Scientific Terms (TEST) and that thesaurus-identified. If it is not possible to select indexing terms which are Unclassified, the classification of each should be indicated as with the title.)

FATIGUE INITIATION

WELDMENTS

HIGH STRENGTH STEEL

SIZE EFFECTS